UNIVERSITY OF ALBERTA
LIBRARY

Regulations Regarding Theses and Dissertations

Typescript copies of theses and dissertations for Master's and Doctor's degrees deposited in the University of Alberta Library, as the official Copy of the Faculty of Graduate Studies, may be consulted in the Reference Reading Room only.

A second copy is on deposit in the Department under whose supervision the work was done. Some Departments are willing to loan their copy to libraries, through the inter-library loan service of the University of Alberta Library.

These theses and dissertations are to be used only with due regard to the rights of the author. Written permission of the author and of the Department must be obtained through the University of Alberta Library when extended passages are copied. When permission has been granted, acknowledgement must appear in the published work.

This thesis or dissertation has been used in accordance with the above regulations by the persons listed below. The borrowing library is obligated to secure the signature of each user.

Please sign below:

Date	Signature	Institution

THE UNIVERSITY OF ALBERTA

A FORCE CONTROL SYSTEM FOR A PHYSIOLOGICAL APPLICATION

A THESIS

SUBMITTED TO THE FACULTY OF GRADUATE STUDIES

IN PARTIAL FULFILLMENT OF THE REQUIREMENTS FOR THE

DEGREE OF MASTER OF SCIENCE

DEPARTMENT OF ELECTRICAL ENGINEERING

By

EDWARD KARPINSKI

EDMONTON, ALBERTA

JUNE, 1966

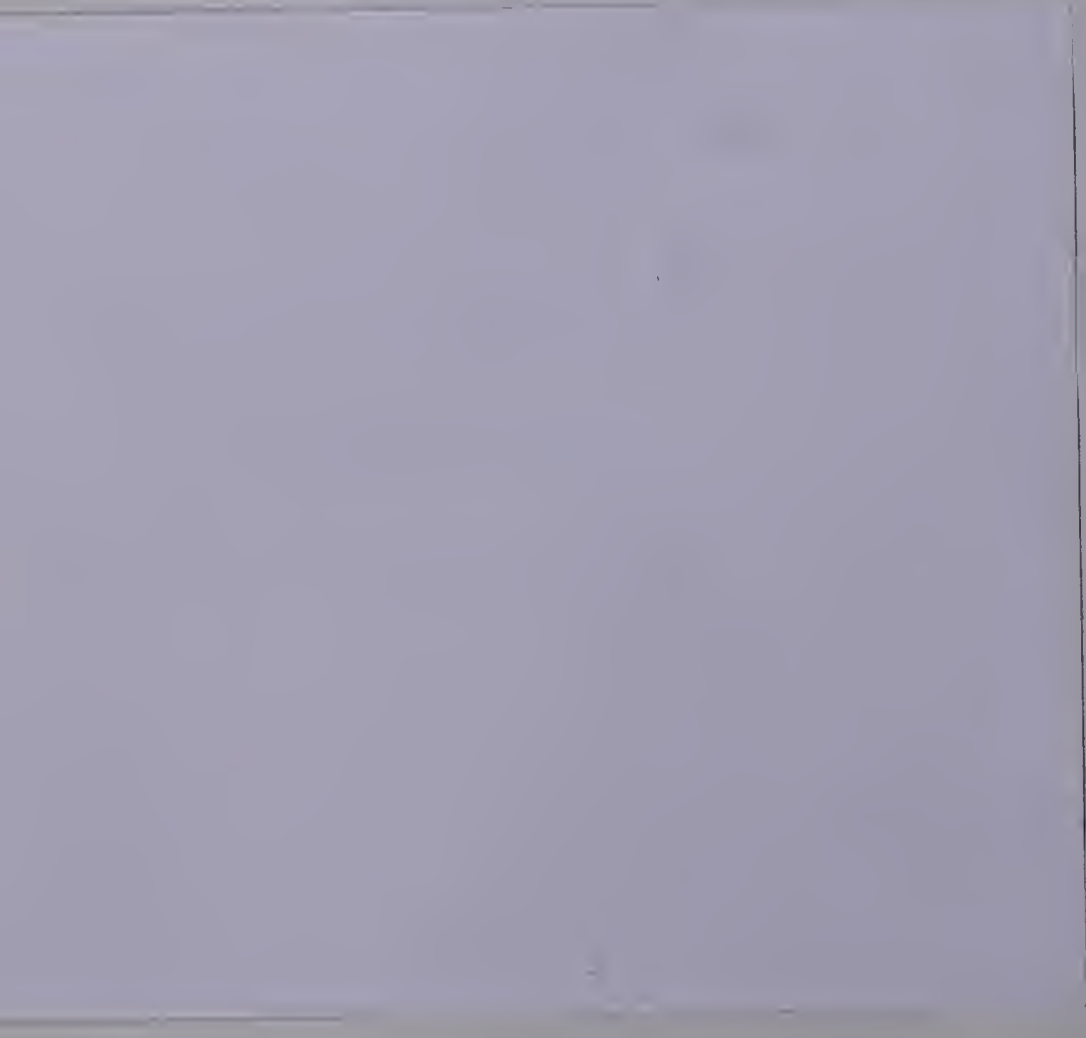

TABLE OF CONTENTS

LIST OF FIGURES

ABSTRACT

In the study of some biological systems, control theory may be applied. To measure the transfer functions of these biological transducers, such as a muscle spindle, a device which produces a force linearly representing an input electrical signal independent of the compliance and damping of the spindle is required. This thesis deals with the design of such a device utilizing a Sanborn pen motor as the force producing device and a force transducer. This system was found to be unstable due to two pairs of complex conjugate poles. The system was compensated in such a way that the effects of the complex poles were almost cancelled. Operation of the system closed loop showed a marked improvement in distortion over open loop operation. The system was then used to apply a sinusoidal force to a preparation of frog muscle in an attempt to determine the mechanical small signal transfer function of whole muscle.

ACKNOWLEDGMENTS

The author wishes to express his appreciation for the encouragement and assistance received during the preparation of this thesis. The work described in this thesis was carried out at the Department of Electrical Engineering, University of Alberta, under the supervision of Professor Y. J. Kingma, to whom the writer wishes to express his sincere indebtedness for advice and assistance throughout the work.

The author would also like to thank Dr. K. M Chapman and Dr. N. Clinch of the Department of Physiology for their co-operation and many helpful suggestions. The author is thankful to the staff and graduate students of the Department of Electrical Engineering for their advice and to his wife, Eileen, for her help in the preparation of this thesis.

The author is further indebted to the Medical Research Council, the National Research Council and the University of Alberta for financial assistance.

CHAPTER I

INTRODUCTION

1.1 PURPOSE

The primary purpose of this project was the building and testing of a control system which would produce a force output linearly representing an electrical input signal. As the force producing device a Sanborn type 51-500 galvanometer was to be utilized. The force sensing device which would monitor the applied force and also provide a correcting signal was to be a Statham type G1-4-250 unbonded strain gauge excited by a Tektronix type 3C66 carrier amplifier. One application of this type of device is in the study of the input versus output characteristic of mechanoreceptors such as muscle spindles and cockroach spines. The input into such a preparation would be the force supplied by the galvanometer; while the output would be the frequency of nerve action potentials. Since muscle spindles are said to be nonlinear with respect to damping and spring constants, the secondary purpose of this project was to attempt to measure the passive transfer function of muscle. Muscle was to be tested rather than spindles due to the difficulty of dissecting the spindles.

1.2 GENERAL

The usefulness of applying various forces to biological preparations such as muscle spindles lies in the fact that physiologists may derive transfer functions relating to the individual preparation; such as in Chapman (3) and Chapman and Smith (4). The transfer function of the mechanoreceptor studied helps in the understanding of the function of the receptor in the maintenance of normal body

function. The usual mechanoreceptors which may be studied in this fashion, such as the spindle from the fourth toe of a frog's leg, are the ones which aid in reflex action. A classical example of reflex action is the simple knee jerk.

The device was designed to facilitate the application of various mathematical forces to the muscle spindle which is the sensing device for the stretch reflex of the fourth toe of a frog's leg. Muscle spindles are bundles of modified muscle fibres called intrafusal fibres. The sensory endings are coiled around a short length of the bundle and are called anulo spiral endings. The muscle spindles lie among the ordinary, or extrafusal, muscle fibres and share their attachments so that they are extended when the muscle lengthens and relaxed when the muscle is shortened. When the muscle is elongated, the sensory portion is deformed resulting in depolarization of the excitable membranes and initiating a set of action potentials. These action potentials are propagated up the group I afferent nerves coming from the anulo spiral endings. The action potentials travel to a synapse in the spinal cord and cause other action potentials to be initiated and propagated down the alpha efferent fibres. These action potentials reach the end-plate region of the muscle and cause depolarization of the membrane which, in turn, causes the contraction of the extrafusal fibres. This type of mechanism has the properties of a length servomechanism; for example, a self-regulating closed-loop mechanism using negative feedback from the spindle to maintain a constant length.

A schematic diagram of a muscle spindle and its attachments is shown in Figure 1.

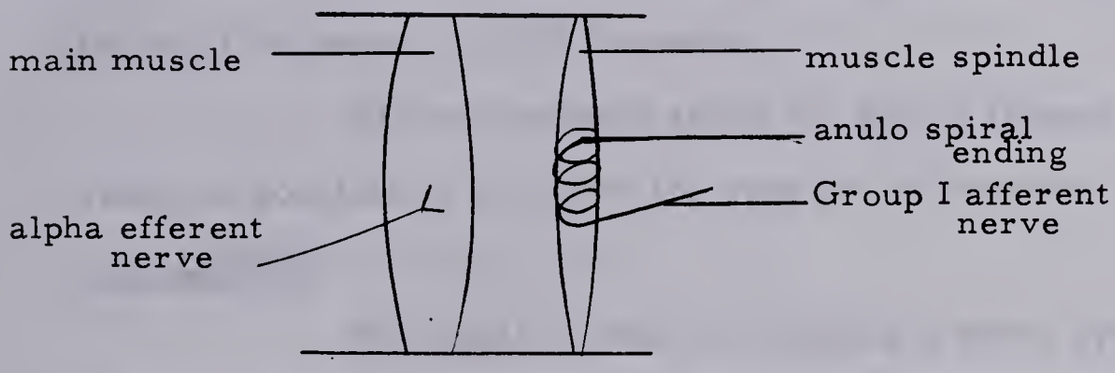

Figure 1. Muscle Spindle

The mechanoreceptor part of the above system consists of only the intrafusal muscle fibres, the deformation sensitive anulo spiral endings and the associated nerve fibres. It may be considered as a type of transducer. The transfer function of such a transducer may be derived in the usual manner of applying a known input and studying the output of the nerve fibre; which in this case is impulse frequency.

The transfer function would be nerve impulses per second divided by the input force or displacement.

1.3 SYSTEM REQUIREMENTS

To facilitate the analysis of such biological preparations the applied force should linearly represent some input signal. This means that applied force should contain as low a percentage of distortion products as possible. This requirement suggests that high system gain and negative feedback must be used to correct for load nonlinearities.

The bandwidth of such a system should extend to nearly one hundred hertz since prior work in the field by Chapman and Smith (4) indicates that useful results may be obtained in that range.

Useful force outputs would vary from 19.6×10^{-5} newtons (20 mg.) to about 9.8×10^{-2} newtons.

The steady state error for such a system should be as small as possible to eliminate the need for calibration.

1.4 DESIGN

The usual method of designing a servo system is to specify the required closed loop response characteristics and desired accuracy; then from these requirements to choose components which will enable the system to meet these specifications. In many, if not all, cases some compromise must be reached between specifications and component costs.

This procedure could not be used in this project since it was specified that some of the available components were to be used. These components were the G1-4-250 Statham unbonded strain gauge, the Tektronix carrier amplifier, and the Sanborn type 51-500 galvanometer.

1.5 THE GALVANOMETER

The galvanometer used in this project was a Sanborn type 51-500 pen motor. It consists of a permanent magnet with a magnetic field strength of .8 weber/m^2. The coil consists of 3,000 turns, is center tapped, and has a resistance of 3,000 ohms. It is suspended in the magnetic field via a torsion rod clamped at one end. The torque produced by the galvanometer is 2×10^{-3} newton meters per ma.

1.6 FORCE TRANSDUCER

The device which was to be used as the force transducer is the Statham type G1-4-250 unbonded constantan strain gauge bridge. The force range of this device is 1.1 newtons in either direction with a maximum excitation of 9 volts. Sensitivity of the strain gauge is 25 microvolts/volts gm. force, while the compliance is .3 mm./kgm. force.

1.7 CARRIER AMPLIFIER

To provide the excitation voltage to the strain gauge and to amplify the output, the Tektronix type 3C66 carrier amplifier was used. This unit is specifically designed for transducer applications. The excitation voltage is in the form of a 25 kilohertz carrier and the bandwidth of this unit is 6 kilohertz. The amplification system is essentially drift-free; therefore the overall system drift is a function of the stability of the external transducer.

In the operation of the unit, the bridge modulates the applied 25 kilohertz carrier in accordance with the bridge unbalance. This bridge unbalance is produced by an input to the transducer which changes the resistances in the bridge. Under no input conditions to the transducer the bridge is balanced and the carrier is suppressed at the output. However, a force input to the transducer causes impedance changes which, in turn, modulate the carrier. This a.c. bridge, which consists of the resistances of the strain gauge and balancing circuit, produces suppressed carrier amplitude modulation.

The modulation side bands from the bridge are applied to an a.c. coupled amplifier where the side bands are amplified while other frequencies are rejected. These side bands are then applied to a phase sensitive demodulator.

The output of the demodulator is filtered and corresponds to the force signal applied to the transducer.

A block diagram of the 3C66 carrier amplifier is shown in Figure 2.

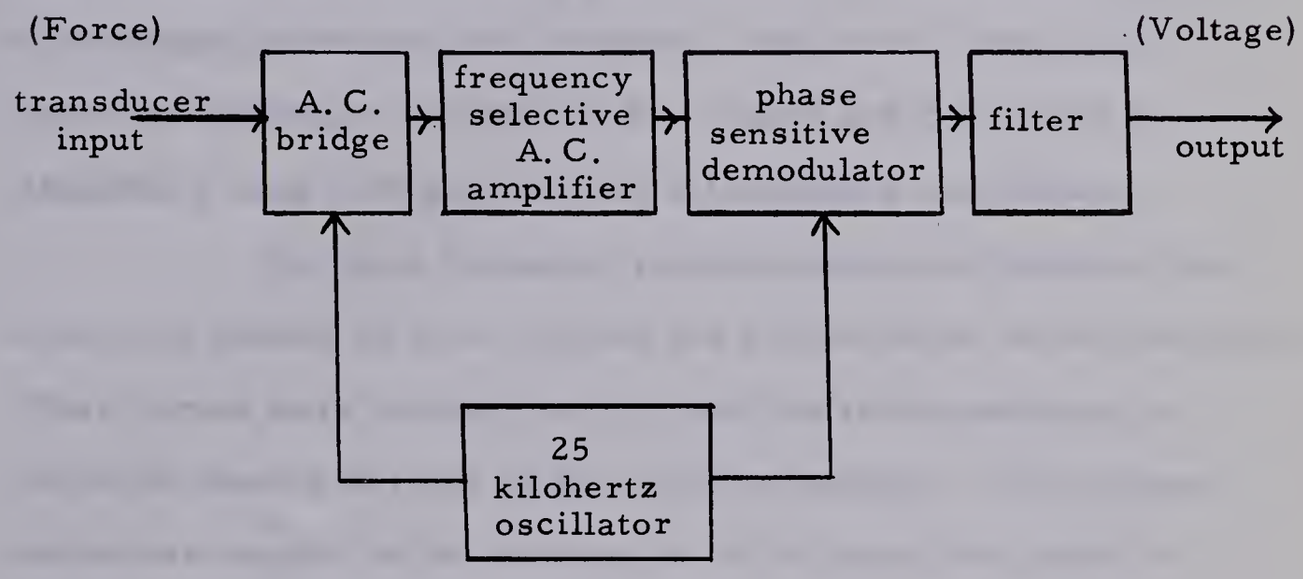

Figure 2. Block Diagram of 3C66 Carrier Amplifier

1.8 SPECIFICATIONS

In the design of this system it was expected that several of the requirements would be subject to limits of equipment. However, several main specifications were suggested as the extreme requirements of the final system. These specifications are as follows:

(1) driving force range 9.8×10^{-5} newtons (10 mg.) to 9.8×10^{-2} newtons (10 gm.) peak to peak force;

(2) bandwidth D. C. to 100 hertz; and

(3) steady state error less than 2 percent.

CHAPTER II

2.1 OPEN LOOP MEASUREMENTS

In order to obtain the characteristics of the system, it was assembled as for normal operation and the frequency response was measured. To drive the galvanometer a driver amplifier with a low output impedance was designed. The circuit was used to obtain the frequency response of the system and it is shown in Appendix I along with gain and output impedance calculations.

The first frequency response curve was obtained with a piece of number 18 wire coupling the galvanometer to the transducer. Other curves were obtained using either the semi-tendinosus or sartorius muscle of frogs as the coupling material. The galvanometer was coupled to the transducer via the muscle in order to monitor the force applied to the muscle. In order to prevent buckling the coupling material was prestretched by a force of about one gram and the applied sinusoidal force was about 9.8×10^{-3} newtons peak to peak.

The experimental arrangements used to obtain the frequency response curves is shown in Figure 3.

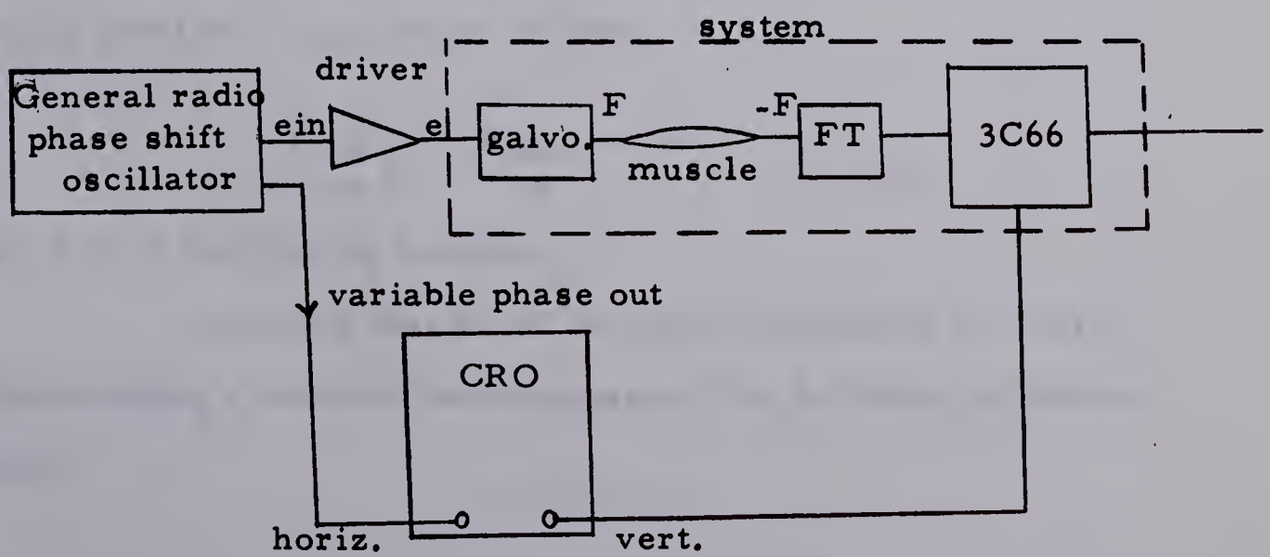

Figure 3. Block Diagram of Experimental Set-up Used to Obtain the Frequency Response Curves of the System

Using the experimental arrangement shown in Figure 3, the open loop frequency response curves shown in Figure 4 were obtained. The curves are plotted with the gain normalized to one.

The shape of the frequency response curves indicates that the system consists of two second order systems in series. Additional information was obtained by applying a step of force to the transducer showing a poorly damped system with a resonant peak of 34 decibels. The damping ratio calculated from the logarithmic decrement was found to be approximately .016. The resonant frequency of this system was measured to be 3,000 radians per second.

The other second order system which occurs at the lower frequency is much better damped. This system consists of the inertia of the galvanometer, the mechanical characteristics of the coupling material and the spring constant of the transducer.

Since the coupling material determines the transfer function of this part of the system, the resonant frequency varies with the coupling as shown in Figure 4.

The differential equation which describes the typical second order system consisting of a mass M, damping B, and a spring constant K is given as follows:

$$M\frac{d^2x}{dt^2} + B\frac{dx}{dt} + Kx = f(t),$$

where f (t) is the forcing function.

Assuming that all of the initial conditions are zero and performing a Laplace transformation, the following equations result:

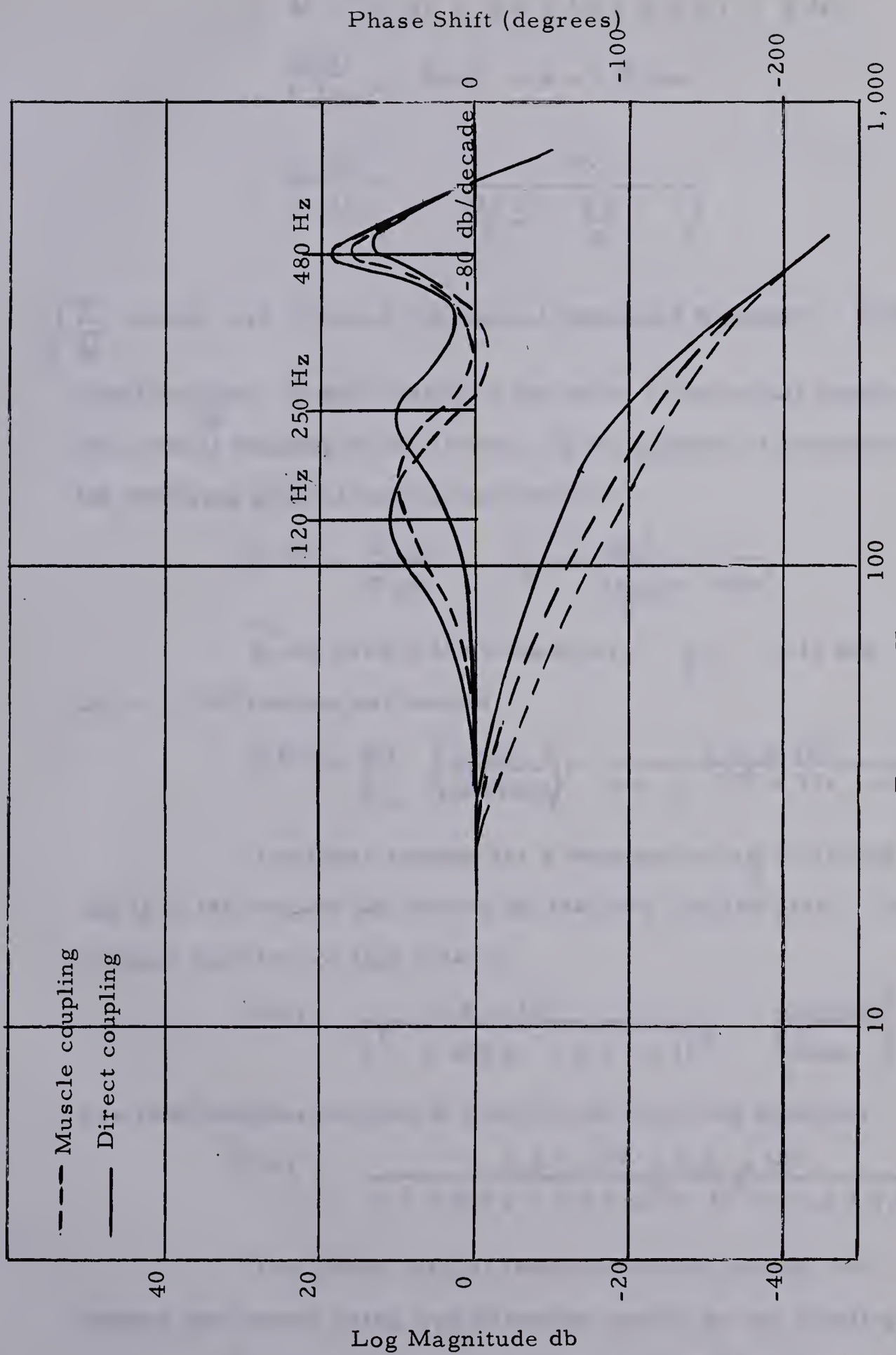

Figure 4. Open Loop Frequency Response Curves

$$M s^2 X(s) + B s X(s) + K X(s) = F(s),$$

$$\frac{X(s)}{F(s)} = M s^2 + B s + K \text{ and}$$

$$\frac{X(s)}{F(s)} = \frac{K}{\left(\frac{M s^2}{K} + \frac{B s}{K} + 1\right)}.$$

$\sqrt{\frac{K}{M}}$ equals ωn which is the natural undamped frequency. B/K is equal to $2\zeta\omega n$. In this case ζ is the ratio of the actual damping to the critical damping of the system. If the equation is normalized the following general expression results:

$$G(s) = \frac{X(s)}{F(s)} = \frac{\omega n^2}{s^2 + 2\zeta\omega n + \omega n^2}.$$

In the case of the transducer, $\zeta = .016$ and $\omega n = 3{,}000$ radians per second.

$$G(s) = \frac{Eo}{F_{in}} \left(\frac{\text{volts}}{\text{newtons}}\right) = \frac{9.0 \times 10^6}{9.0 \times 10^6 + 97s + s^2.}$$

The other system has a damping ratio ζ of .25 and ωn is 1,380 radians per second for the wire coupled case. The transfer function for this case is:

$$G(s) = \frac{1.8 \times 10^6}{s^2 + 690 s + 1.8 \times 10^6} \left(\frac{\text{newtons}}{\text{volts}}\right).$$

The total transfer function is given by the following equation:

$$G(s) = \frac{1.8 \times 10^6 \times 9.0 \times 10^6}{(s^2 + 690 s + 1.8 \times 10^6)(s^2 + 97 s + 9.0 \times 10^6)}.$$

The lowest natural frequency measured was 750 radians per second using frog sartorius muscle as the coupling material. Changing the coupling resulted in very little change in damping ratio.

The denominators were factored resulting in two pairs of complex conjugate poles for the direct coupled case given below as:

$$G(s) = \frac{16.2 \times 10^{12}}{(s-49.0+j3000)(s-49.0-j3000)(s-345+j1295)(s-345-j1295)}$$

and for the sartorius coupled case as:

$$G(s) = \frac{5.25 \times 10^{12}}{(s-49+j3000)(s-49-j3000)(s-187+j720)(s-187-j720)} .$$

Using the above information the root locus diagram shown in Figure 5, was drawn.

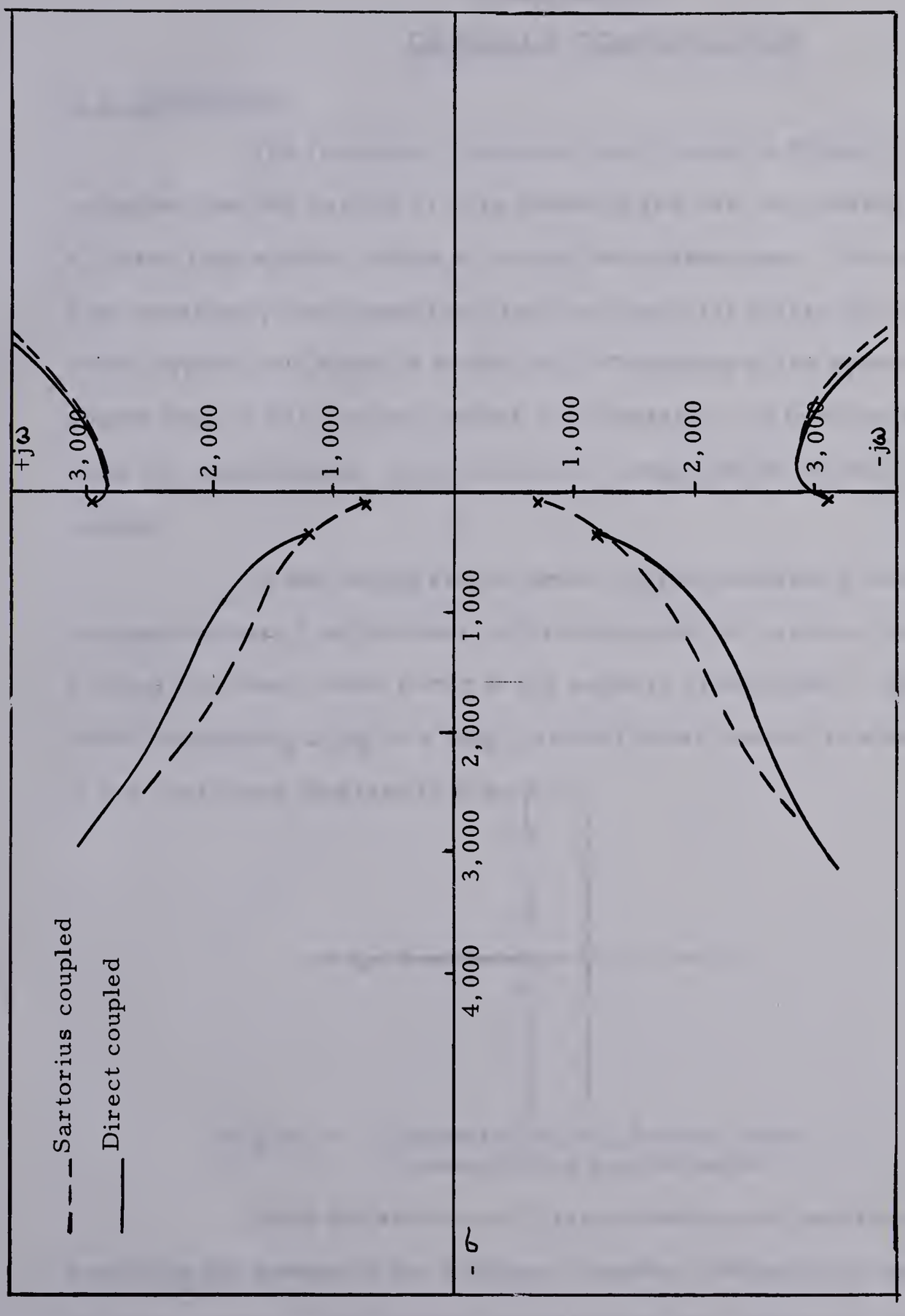

Figure 5. Root Locus Diagram

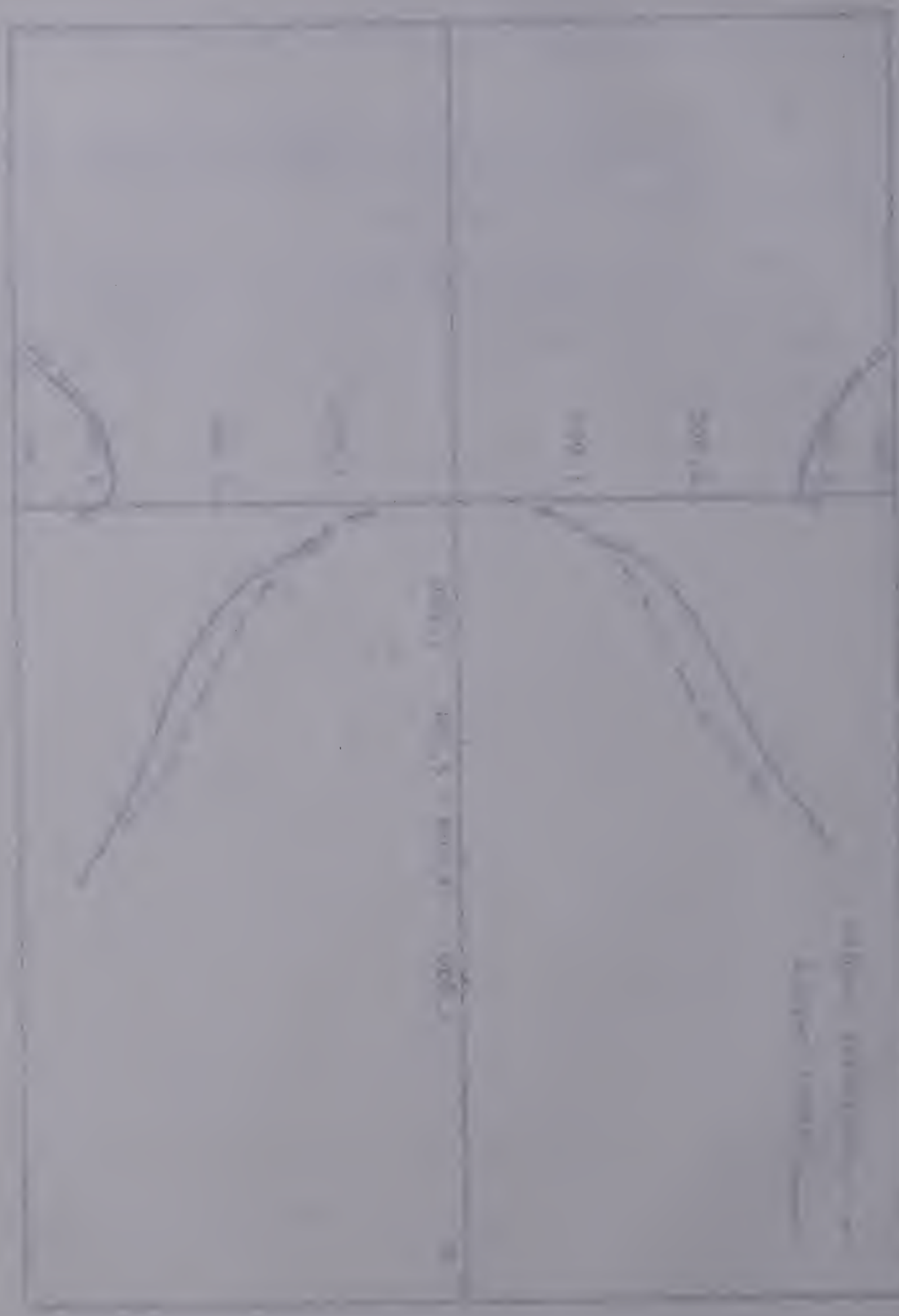

CHAPTER III

DESIGN OF COMPENSATION

3.1 GENERAL

The frequency response curve shown in Figure 4 indicates that the system is very unstable and will not operate as a closed loop system except at a very low system gain. The static loop sensitivity calculated from the root locus for stable operation of the system was found to be $K < .003$. Operation of the system closed loop at this low gain offers no advantage, and in order to meet the specification, some method of compensation must be applied.

In any single second order system containing complex conjugate poles; a lag network will compensate the system, improving the steady state error at the expense of bandwidth. The effect of applying a lag to a single second order system is shown in the root locus diagram in Figure 6.

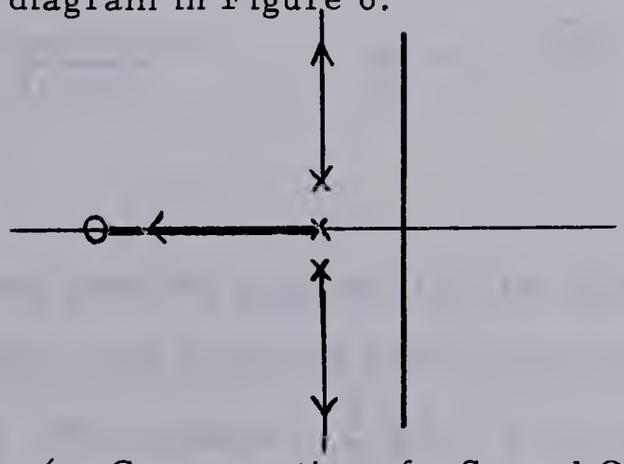

Figure 6. Compensation of a Second Order System with a Lag Network

Since the addition of a lag network to an underdamped second order system is not adequate, another method of compensation must be applied. This method must in some way cancel out the effects of the complex conjugate poles. Cancellation of these unwanted poles may be carried out by the addition of a bridged-T

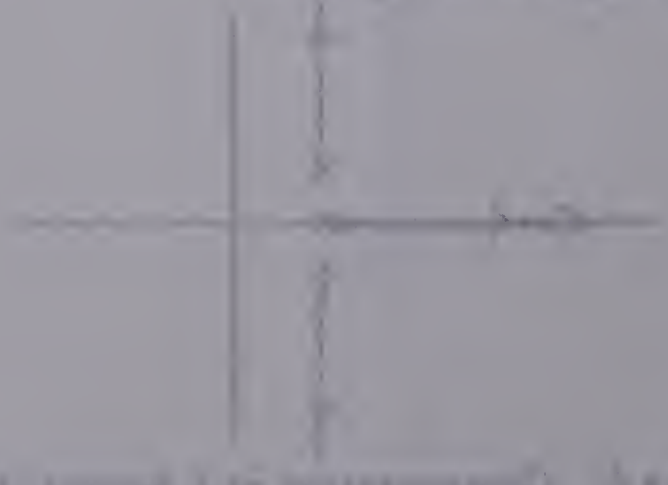

network. This method of compensation is described in Kuo (11) and Chandaket and Rosenstein (5) . The voltage transfer function of a bridged-T network assuming a zero source impedance and an infinite load impedance is given by the following equation:

$$G_c(s) = \frac{s^2 + 2\zeta_1 s\omega + \omega^2}{s^2 + 2\zeta s\omega + \omega^2} .$$

A bridged-T network is shown in Figure 7.

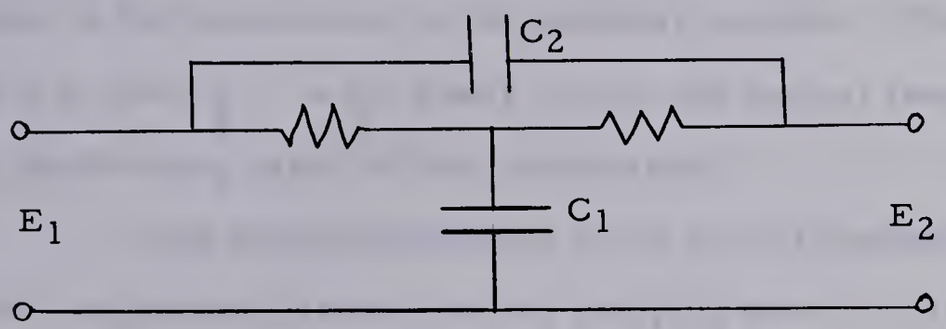

Figure 7. Bridged-T Network

The voltage transfer function given in terms of circuit components is given as follows:

$$\frac{E_2(s)}{E_1(s)} = \frac{1 + 2RC_2 s + R^2 C_1 C_2 s^2}{1 + R(C_1 + 2C_2)s + R^2 C_1 C_2 s^2} ;$$

where $\omega = \frac{1}{R\sqrt{C_1 C_2}}$, $\zeta = \sqrt{\frac{C_2}{C_1}}$, and

$\zeta_1 = \frac{1 + 2\zeta^2}{2\zeta}$.

It is seen from the equations that the zeros may be either real or complex. The poles are always real since $\zeta > 1$ for all values of ζ . For example, $\frac{d\zeta_1}{d\zeta} = 0$ at $\zeta = \frac{1}{\sqrt{2}}$ where $\zeta_1 = \sqrt{2}$. This places the poles in a more desirable location in the s-plane.

Since the system contains two pairs of complex conjugate poles, one bridged-T compensator must be designed so as to cancel the poles representing the force transducer.

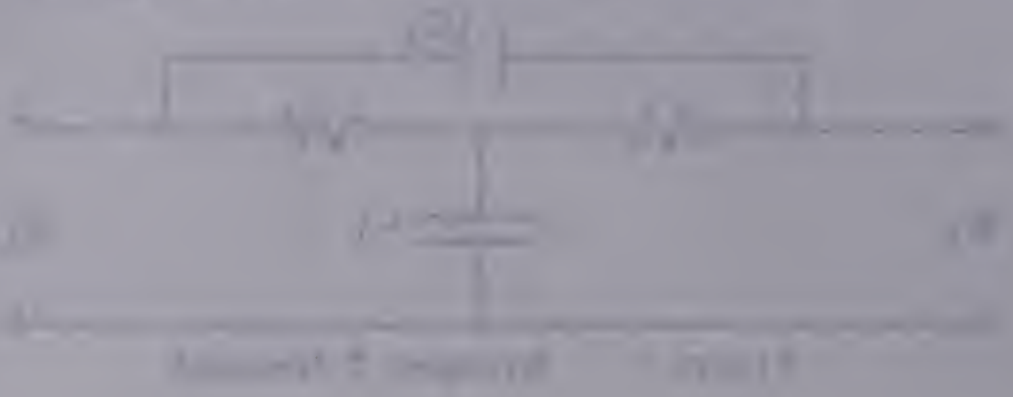

Complete cancellation is difficult and not necessary since the transient terms due to the closed loop complex dipole will be small if cancellation is incomplete.

3.2 DESIGN OF COMPENSATOR FOR THE FORCE TRANSDUCER

To design a compensator which cancels the unwanted poles of the force transducer, the numerator of the compensator must be equal to the denominator of the transfer function. This sets $\omega_c = \omega_n$ and $\zeta_c = \zeta$ where ω_c is the natural frequency and ζ_c is the damping ratio of the compensator.

The natural frequency of the force transducer is equal to 3,000 radians per second and the damping ratio is .016. Since the compensator was designed for approximate cancellation, ω_c was set equal to 3,000 radians per second, and ζ was set equal to approximately .05. This results in the following equations: $3{,}000 = \frac{1}{R\sqrt{C_1 C_2}}$ and $.05 = \sqrt{\frac{C_2}{C_1}}$. The solution of these equations, which involves picking a value for R and solving for C_1 and C_2, resulted in $C_1 = .5$ uf, $C_2 = .001$ uf and $R = 15$ K. The nearest commercially available value of $C_1 = .47$ uf was chosen. These component values result in $\omega_c = 3{,}100$ radians per second and $\zeta = .046$ and give the following transfer function:

$$G_c(s) = \frac{s^2 + 285s + 9.3 \times 10^6}{s^2 + 6{,}700s + 9.3 \times 10^6} .$$

The transfer function of the bridged-T network was factored and the root locus diagram was plotted.

The root locus diagram shown in Figure 8 represents the system compensated with a single bridged-T network. Stability of the system was not improved. Static loop sensitivity for stability was calculated from the root locus to be $K < 3.4 \times 10^{-3}$ which is the value of K on the imaginary axis of the root locus. Figure 11 shows the effect of the compensator on the system in terms of frequency response. For a system gain of about one, the system with the direct coupling will be stable.

3.3 DESIGN OF A BRIDGED-T NETWORK TO COMPENSATE THE SECOND PAIR OF COMPLEX CONJUGATE POLES

Since the addition of a single bridged-T compensator to the system showed insufficient improvement in system statility, another bridged-T network was added to the system. This compensator would have its zeros placed so it would have the maximum effect on the two complex conjugate poles which are dependent on the coupling material. A damping ratio for the compensator of .5 and a natural frequency of 1,000 radians per second were chosen.

Solution of the equations, as in the previous case, resulted in the following component values: $C_2 = .1$ uf, $C_1 = .33$ uf and $R = 5.6$ K. These component values resulted in the following transfer function which is given in factored form:

$$G_c(s) = \frac{(s + 540 - j820)(s + 540 + j820)}{(s + 2,460)(s + 400)}.$$

The result of this additional compensation is shown in the root locus diagram in Figure 9, and in the frequency response curve in Figure 11. For the system to be stable the static loop sensitivity was found to be $K < .41$. For stability the system gain from the frequency response curve was about 3.1.

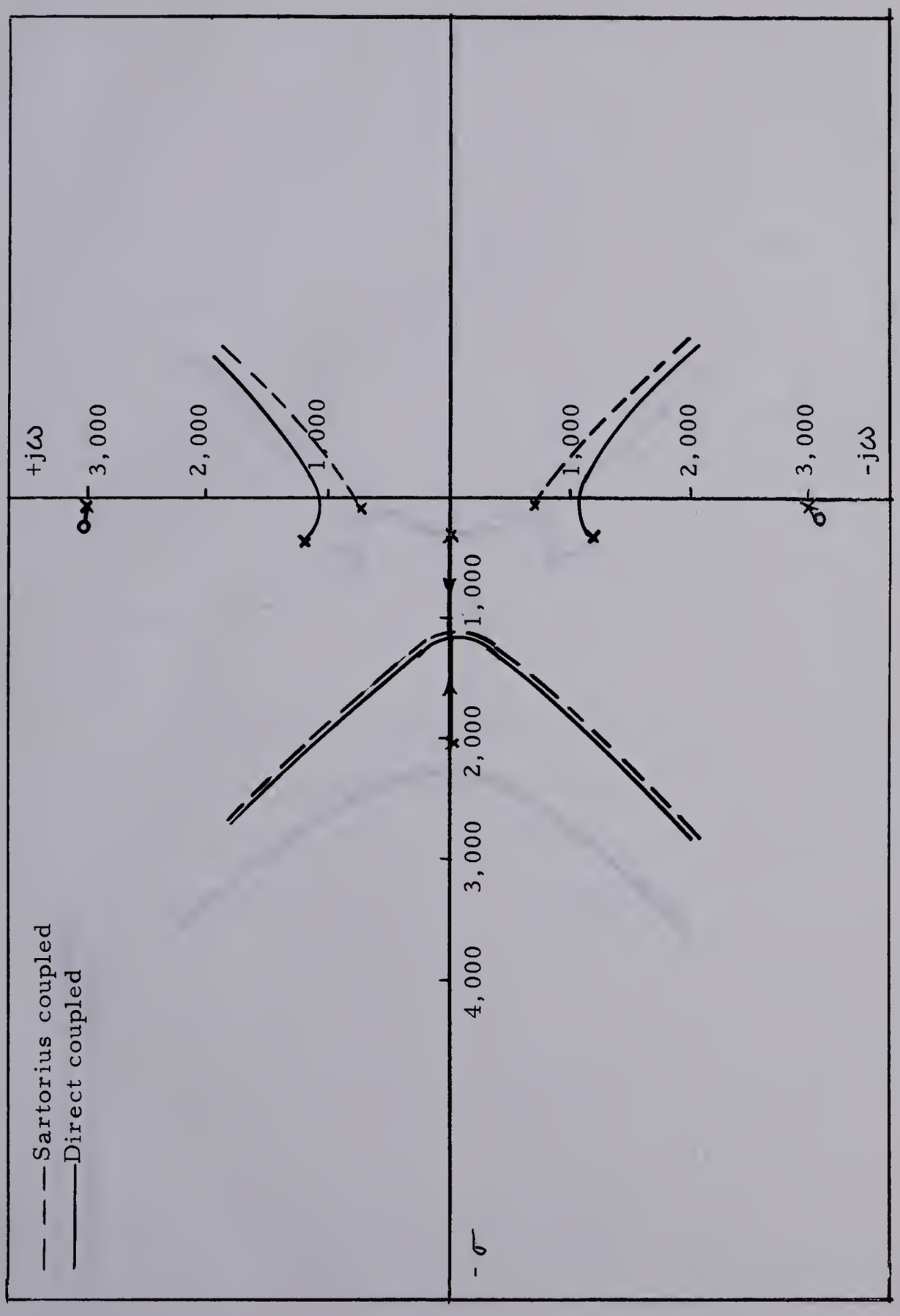

Figure 8. Root Locus Diagram Showing the System Compensated With a Bridged-T Network

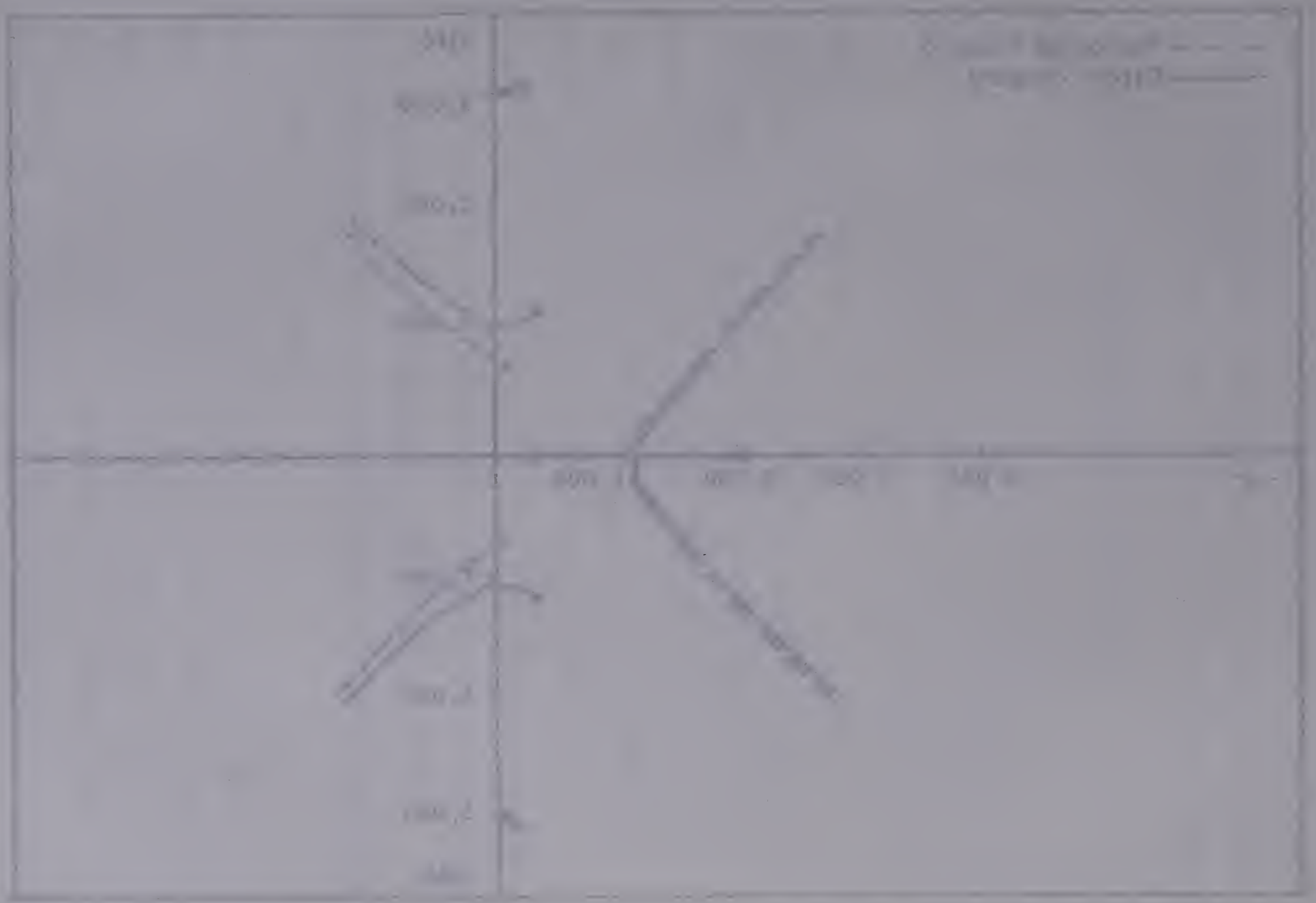

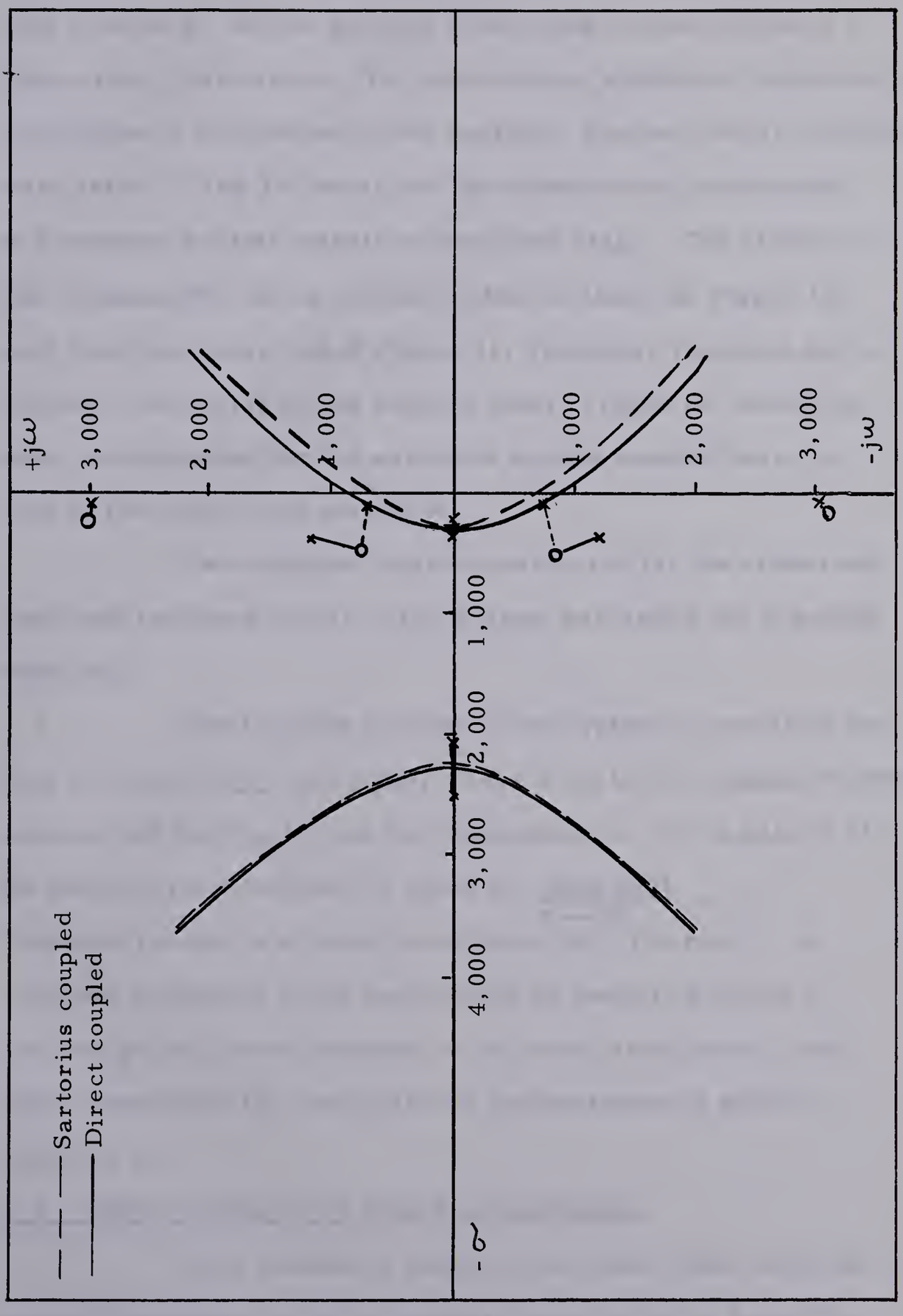

Figure 9. Root Locus Diagram Showing the Effect of Two Bridged-T Compensators on the System

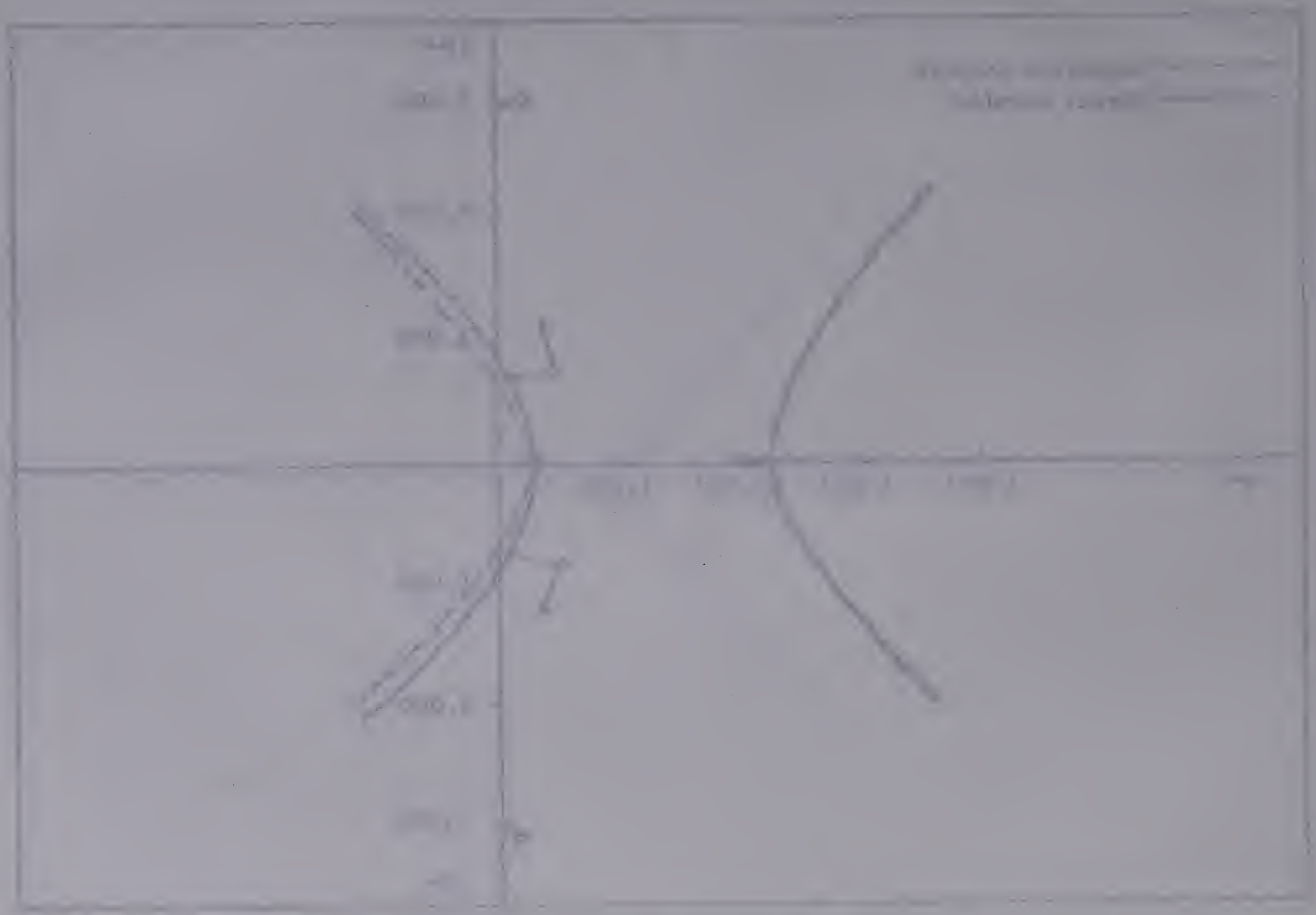

3.4 DESIGN OF LAG COMPENSATOR

For stability of the system the maximum allowable gain is about 3. At this gain the closed loop system will have a large steady state error. To improve this, additional compensation in the form of a lag network was applied. The two corner frequencies were set at 23 and 330 Hertz and the network was incorporated in a common emitter transistor amplifier stage. The effects of this compensator on the overall system is shown in Figure 10, root locus diagram, and in Figure 11, frequency response curve. Figure 11 shows the direct coupled case. Figure 12 shows the same compensation for the sartorius muscle coupled case, as well as the closed loop response.

Two different muscles were used for the closed and open loop response curves. The system was stable for a gain of about ten.

The transfer function of the system is now given by: $K_A G(s) G_{1C}(s) G_{2C}(s) G_{3C}(s)$, where $G(s)$ is the original transfer function and the $G_{nc}(s)$ are the compensators. For a gain of 12 the static error coefficient is given as $\lim_{s \to 0} G(s) = 12$. This gain results in a steady state error of 7.7 percent. A complete evaluation of the system will be made in Chapter 6. The design and circuit diagram of the actual solid state circuit which represents the amplifier and compensators is given in Appendix II.

3.5 IMPROVEMENT OF SYSTEM RESPONSE

In an attempt to improve the steady state error the corner frequencies of the lag network were moved to lower frequencies. The transfer function of the lag network is now

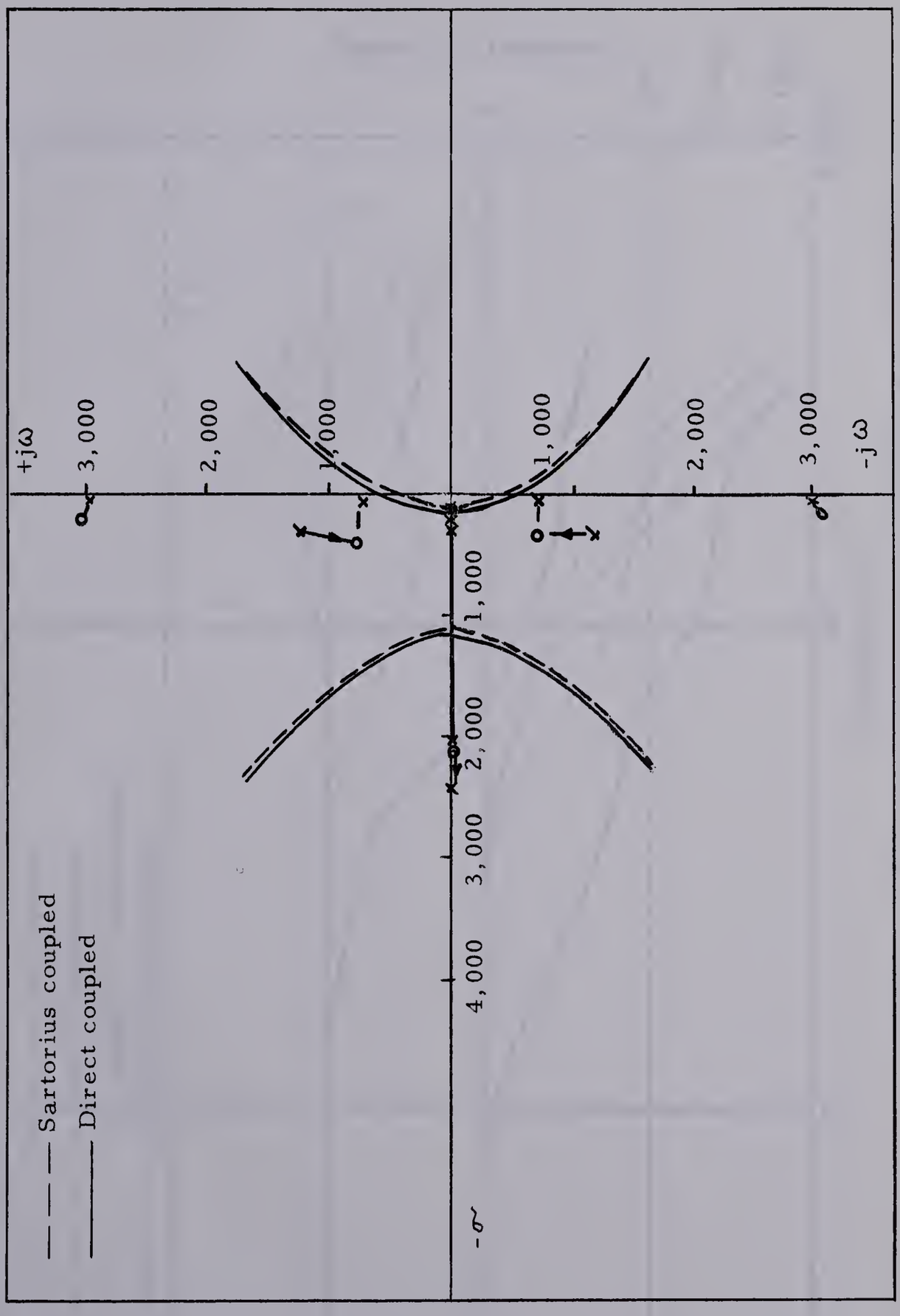

Figure 10. Root Locus Diagram Showing the Effects of Two Bridged-T and a Lag Compensator on the System

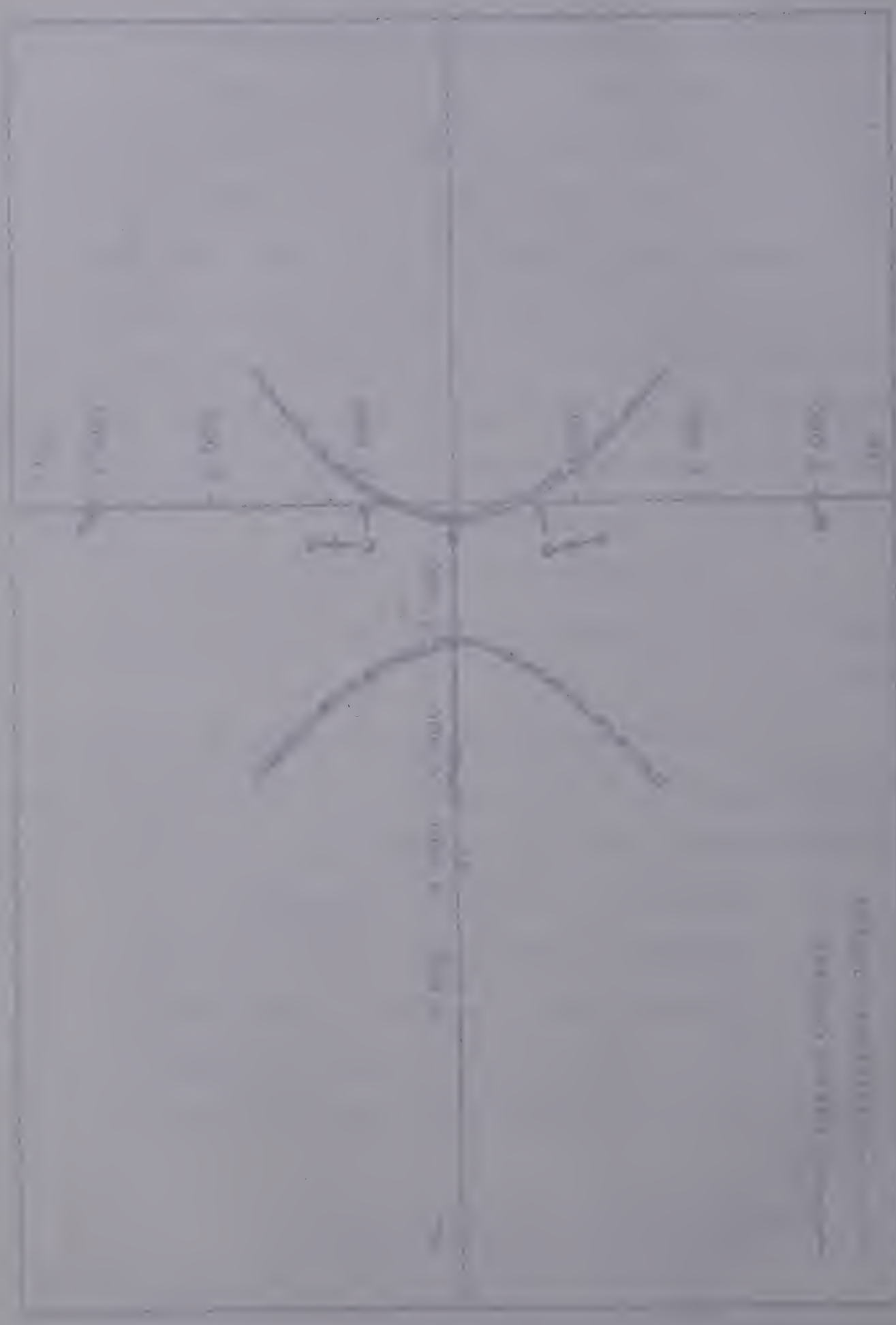

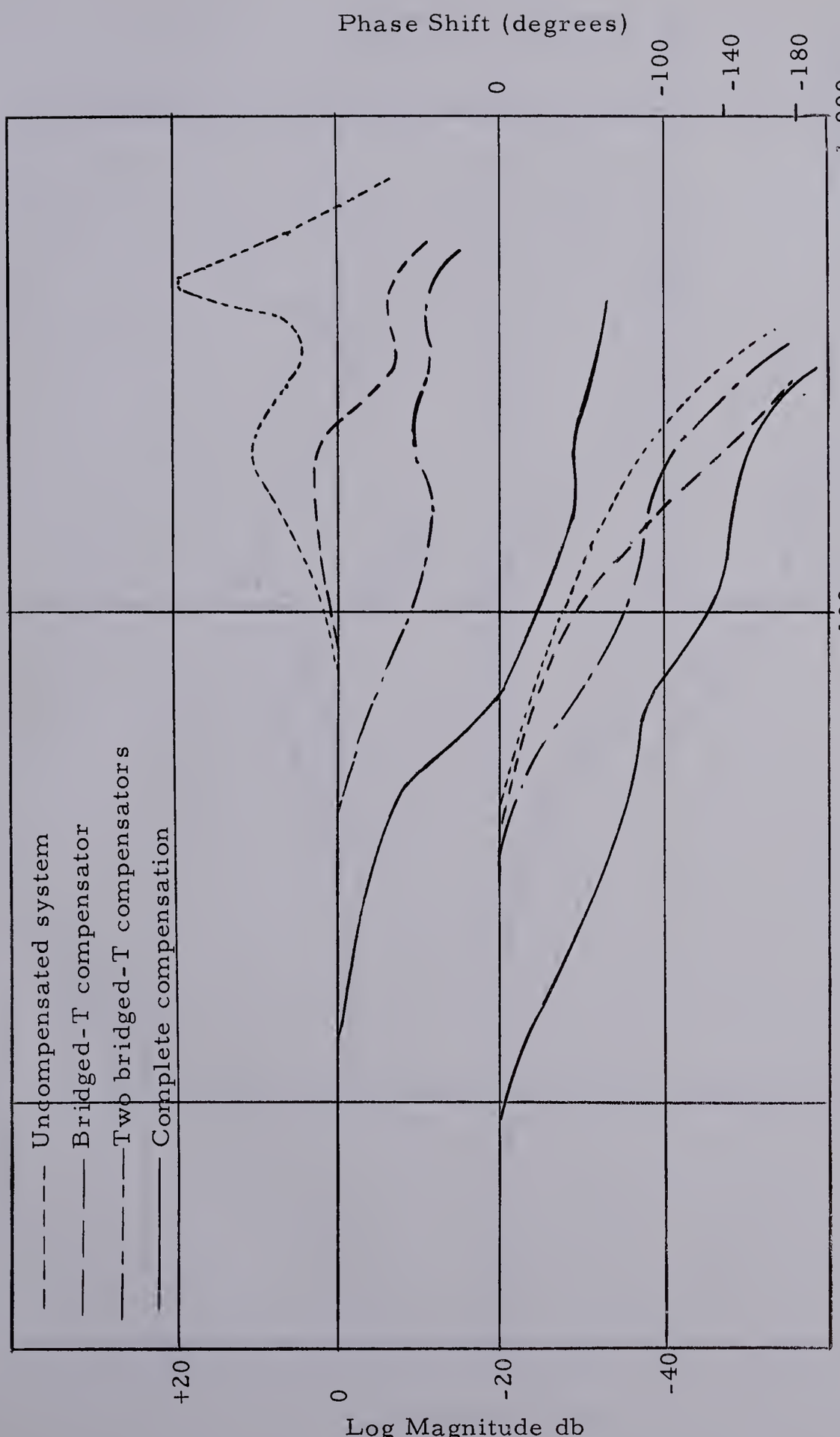

Figure 11. Frequency Response Curves Showing the Effect of Compensation (direct coupled system)

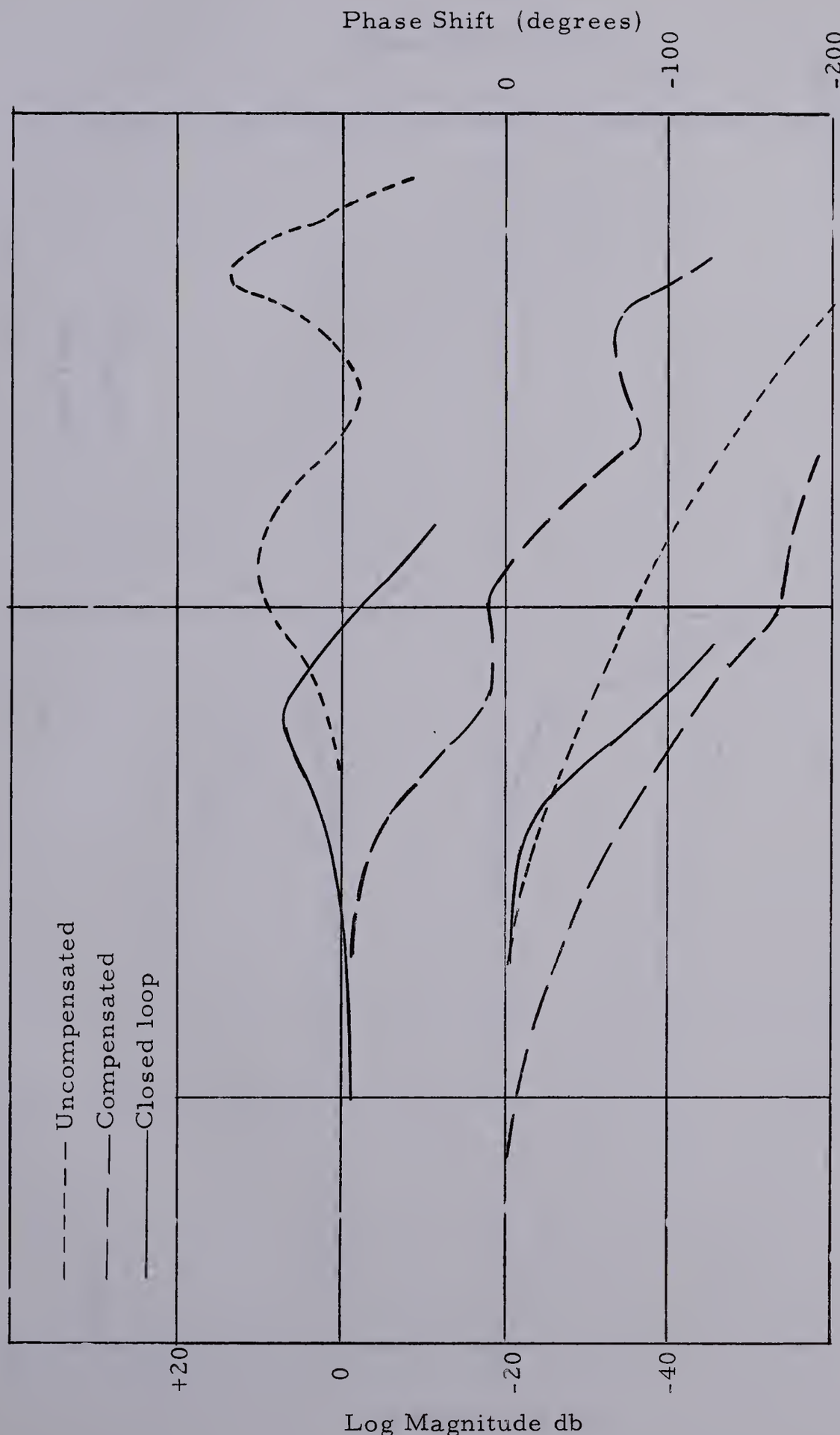

Figure 12. Frequency Response Curves Showing the Open Loop and Closed Loop Response for the Muscle Coupled System

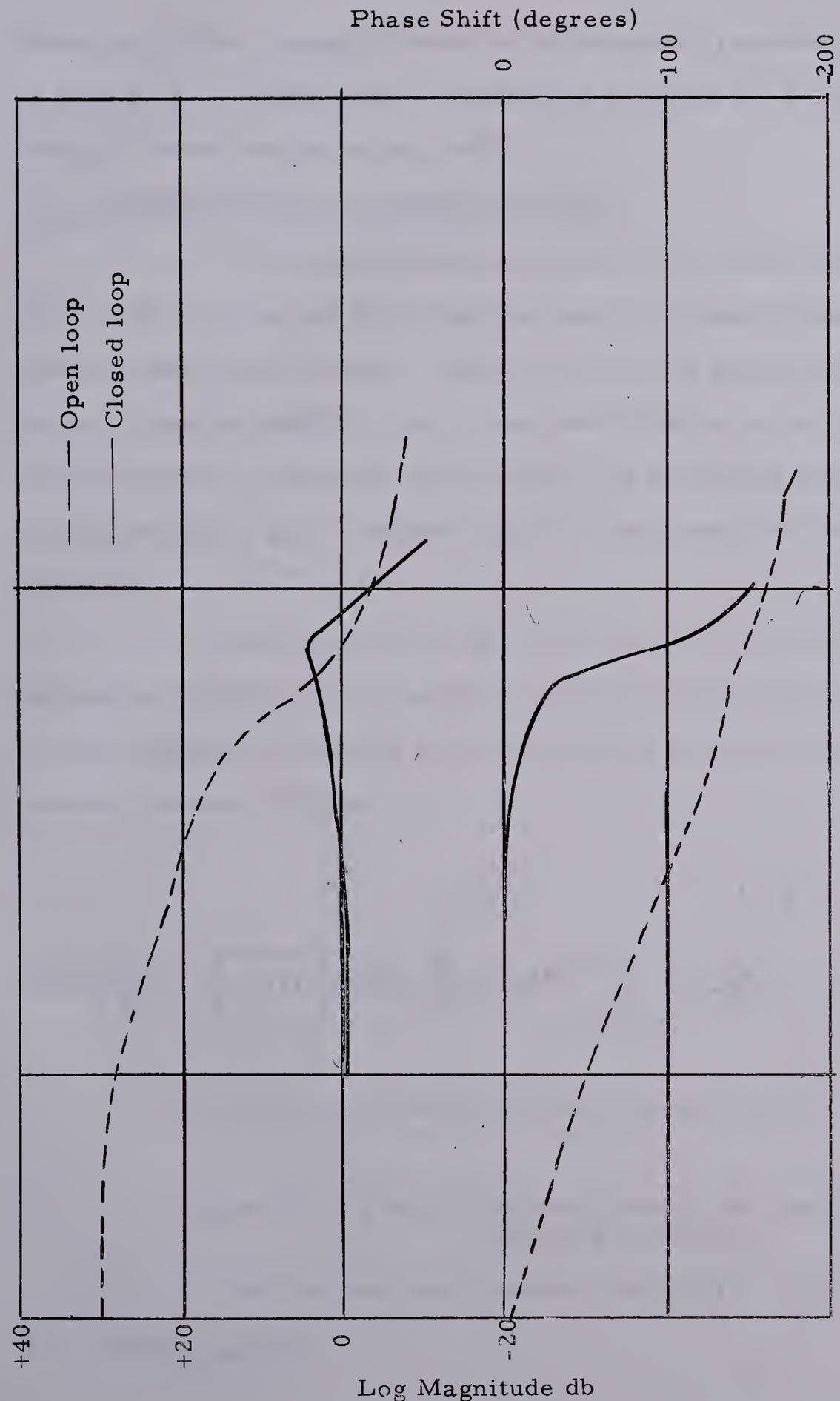

Figure 13. Frequency Response Curves for the Open Loop and Closed Loop System with the Corner Frequency of the Lag Network Moved to 10 Hz

$$G_c(s) = \frac{(s + 1,000)}{(s + 63)}.$$

The effect of this change is shown in the frequency response curve in Figure 13. For the direct coupled case at a gain of 14 the phase margin is measured to be about 40°.

3.6 MINIMIZATION OF DISTURBANCES

In the operation of the system at low force levels, in the order of 30 to 50 mg.,it was noted that excessive noise existed making work at these levels useless. The majority of the noise came from the 3C66 carrier amplifier due to imperfect filtering of the carrier and harmonics. The output level of noise did not depend on the carrier amplifier gain. Another form of noise came from building vibration.

To minimize the effects of these two sources of extraneous disturbances, a method of gain distribution was used. A block diagram showing the disturbances with respect to the system is shown in Figure 14.

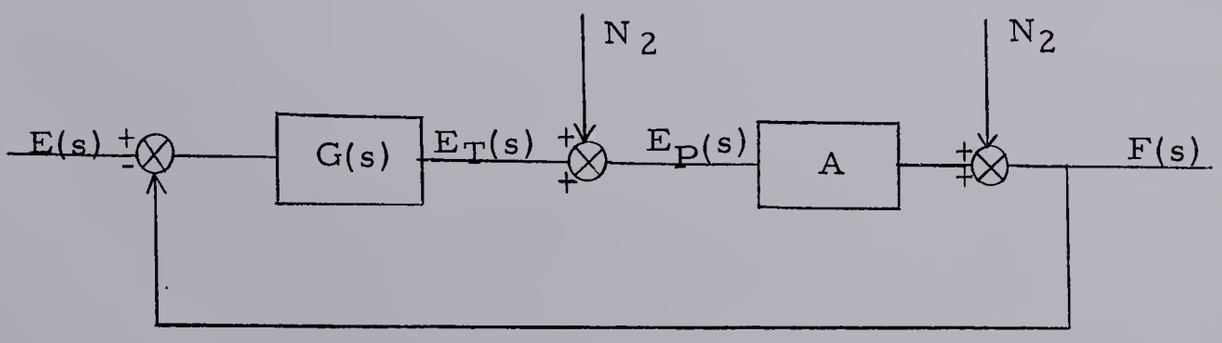

Figure 14. A Block Diagram Showing the Disturbances Affecting the System

For the first case consider that if $N_1 = N_2 = 0$, then

$$F(s) = \frac{AG(s) \quad E(s)}{1 + AG(s)}.$$

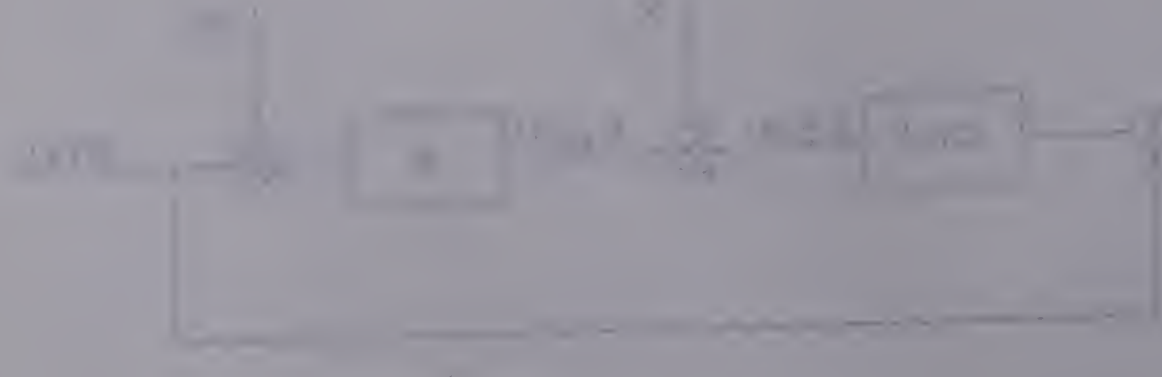

If $E(s) = 0$, $N_1 \neq 0$, and $N_2 = 0$; then $F(s) = \frac{NA}{1 + AG(s)}$.

Therefore, in order to minimize the effects of N_1, the ratio, $\frac{N_1}{G(s)\ E(s)}$, must be made as small as possible.

To minimize the effects of N_2 the ratio of $\frac{N_2}{AG(s)\ E(s)}$ must be minimized. In the actual system this was achieved by having a high gain in the forward amplifier stage. The gain of the carrier amplifier was made very high and the output attenuated so that the disturbance, which was independent of gain, was attenuated by some factor.

In the final design a selector switch was inserted at the output so that the gain of the carrier amplifier could be maintained at the required levels for total system gain by the adjustment of carrier amplifier gain and attenuation.

CHAPTER IV

MEASUREMENT OF MUSCLE TRANSFER FUNCTION

4.1 OBJECT

The secondary objective of this project was to use the servo system, as designed in the first part, to define the biological load; i.e., to measure the passive mechanical transfer function of skeletal muscle. This study was carried out on the striated or skeletal muscle of frogs.

4.2 MUSCLE PHYSIOLOGY

Striated muscle consists of individual fibres which are ten to one hundred microns in diameter. The individual fibres are surrounded by a polarized membrane, the inside of which is about one hundred millivolts negative with respect to the outside.

Each fibre is made up of a number of parallel elements about one micron in diameter which are called myofibrils. The myofibrils themselves, are made up of parallel actin and myosin filaments in a regular array. The myosin filaments are about one hundred and sixty angstroms in diameter and about one or two microns in length. The actin filaments are about one micron in length and fifty to seventy angstroms in diameter. The overlap between the arrays of actin and myosin give rise to the regular pattern of striations as viewed under a microscope. A schematic illustration of a myofibril is shown in Figure 15.

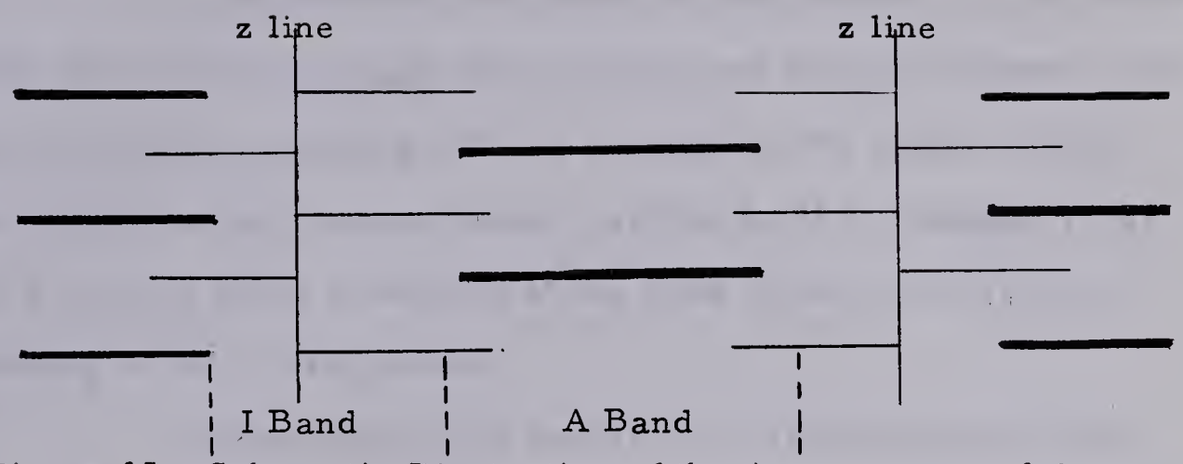

Figure 15. Schematic Illustration of the Arrangement of the Actin and Myosin Filaments in a Myofibril. (The thick filaments are myosin and the thin filaments are actin).

The pattern shown in Figure 15 is characterized by a succession of bands (dense bands called A bands and light bands called I bands). The z line is a narrow structure to which the actin filaments are attached. It has been reported by H.E. Huxley (7) (8) that cross bridges exist between the thick and thin filaments which are the only mechanical linkage between the filaments.

Contraction of muscle is preceded by depolarization of the membrane. This depolarization causes the release throughout the fibre of an activating substance which is now accepted to be calcium ions. The release of calcium enables one of the proteins, myosin, to act as an enzyme and split a phosphate group from adenosine triphosphate (ATP) which provides the energy for contraction. Adenosine triphosphate is a high energy active phosphate compound which, by losing one of its phosphate groups, becomes adenosine diphosphate (ADP) to supply energy to drive chemical reactions which otherwise would not proceed.

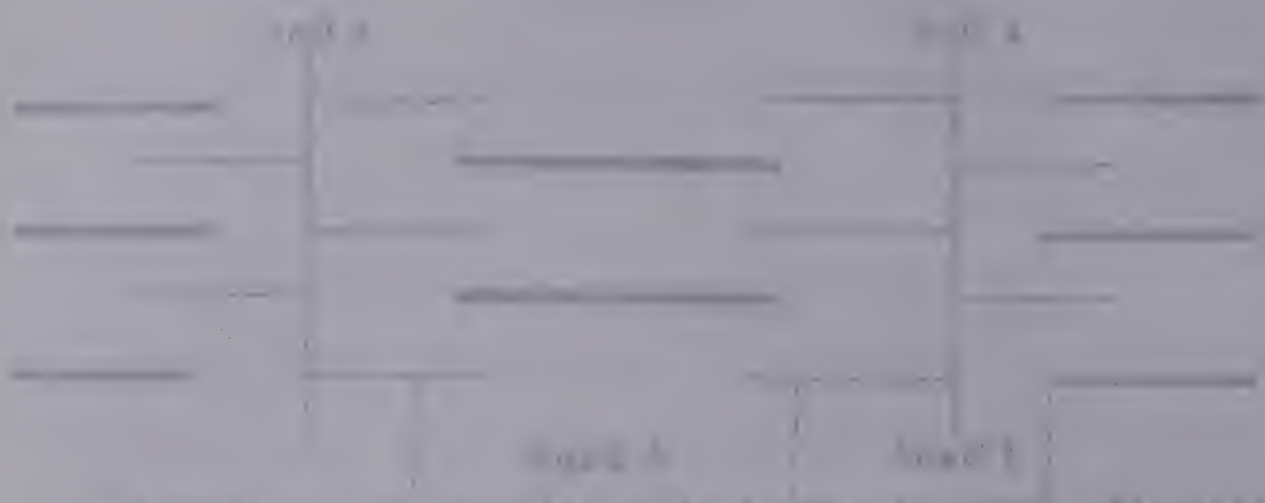

The complete mechanism of contraction is by no means clear, but it is now thought that the actin and myosin filaments slide past each other producing changes in length of the fibre. It has been suggested,and to some extent verified by H.E. Huxley (7) (8) that a relative force is exerted at the sites of the cross bridges resulting in this sliding action.

Mechanically, the result of a striated muscle being stimulated is a "twitch", which is characterized by a phase of contraction, followed by a phase of relaxation. If the muscle is held at a fixed length a tension change will be recorded during the twitch. If the muscle is stimulated again before it has completely relaxed the second contraction will be superimposed on the first contraction. Rapid stimulation which does not allow the muscle to relax results in prolonged mechanical response called a tetanus.

It is generally accepted (10) (12) that active muscle consists of a passive elastic component and a contractile component in series. The contractile component consists of a parallel combination of damping and elastic components. The series elastic and parallel damping component tend to distort the rapid changes in tension.

Two possible mechanical models of muscle in the active state have been proposed by Jewell and Wilkie (10).

In the unexcited state muscle also contains the series elastic component (12). The parallel elasticity and damping exist but probably bear little or no relation to these components in the

active state (2). In whole muscle the membranes would tend to contribute to the damping and compliance.

4.3 GENERAL

Since a muscle is part of the overall control system, it would be useful to describe it in terms of a mechanical transfer function. The knowledge of the transfer function of the coupling material would aid in the determination of overall system stability and it would contribute some information about the properties of passive muscle.

Although skeletal muscle is studied in this case, it is not necessarily mechanically equivalent to the muscle spindle. Skeletal muscle, however, is the best alternative to the muscle spindle and much easier to work with and dissect out.

4.4 PROCEDURE

The usual method of analysis of a mechanical system consisting of mass, damping and compliance is to state the displacement at some point as the output with force as the input. The transfer function is given as $\frac{X(s)}{F(s)}$ where X(s) and F(s) are the Laplace transforms of the displacement and force respectively. This relation, of course, assumes a linear transfer function. Previous work by Buchthal (2) indicates that a linear relation may be obtained for single and small bundles of fibres if small variations of force are used. From this it is clear that in order to obtain a transfer function of whole muscle, a known force must be applied

to a muscle and the displacement measured.

4.5 FORCE MEASUREMENT

The Statham G1-4-250 force transducer was used to monitor the force applied to the muscle. If the mass of the muscle is small, an equal and opposite force appears at the transducer, monitoring the force applied by the galvanometer. In this way, the force applied by the galvanometer may be monitored until the force due to the mass and acceleration of the muscle, introduces a phase lag between the applied and measured force. This effect depends on the effective mass and the compliance of muscle; thus if the measurements are made at frequencies below the resonant frequency of the muscle, little or no error is introduced in the measurement of the force.

4.6 DISPLACEMENT MEASUREMENT

The displacements, or length changes, of the muscle were measured using a light beam lever as shown in Figure 16.

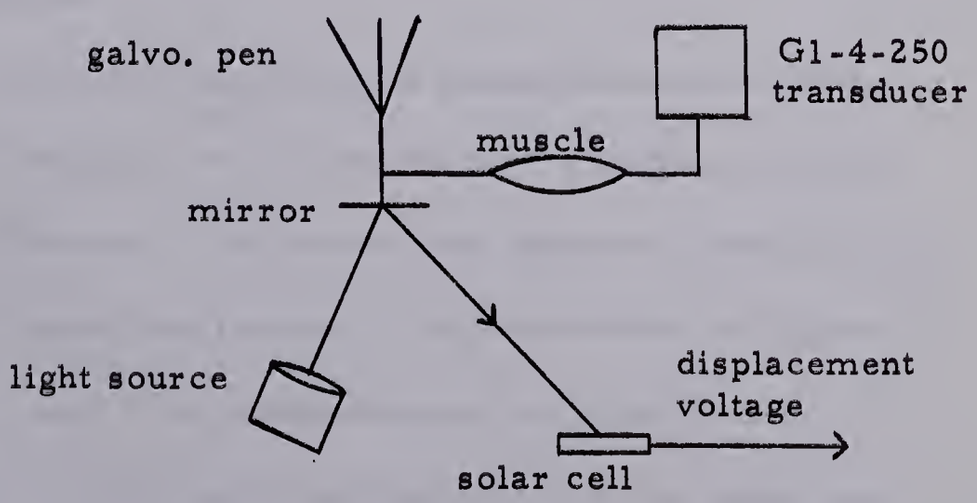

Figure 16. Displacement Measurement System

The light source was focused on a light mirror attached to the galvanometer pen and reflected on to a solar cell, so that changes in the length of the muscle resulted in changes in the area of the solar cell illuminated. The rise time of the solar cell is given as 20 microseconds. The system was calibrated against a dissecting microscope which measured the displacement directly.

4.7 PROCEDURE

The muscle was dissected from freshly killed frogs and the tendons were tied with steel wire and attached via this wire to the galvanometer and the force transducer. The sartorius and semi-tendinosus muscles of frogs were used. In one case the semi-tendinosus muscle of a toad was used. During the test the preparation was kept moist by continual application of Ringer's solution. The measurements were made on muscles weighing 250 mg. or less. The toad semi-tendinosus muscle weighed 250 mg. and had an estimated resonant frequency of about 200 hertz.

Using the experimental arrangement described, the frequency response was measured over a frequency range from .01 to 100 hertz. The system was operated closed loop and exhibited the closed loop frequency response shown in Figure 13 (wire coupled case). The measurements were independent of system characteristics due to the fact that both the output and input were measured. The magnitude of the force applied was kept

constant over the range of measurement to eliminate errors due to the nonlinearity of compliance of the muscle. This was done by varying the input voltage which provided the reference input to the control system. The relative magnitudes of input (reference), force out, displacement and the phase shifts of the outputs were measured as in Chapter II.

A diagram of the experimental arrangement is shown in Figure 17.

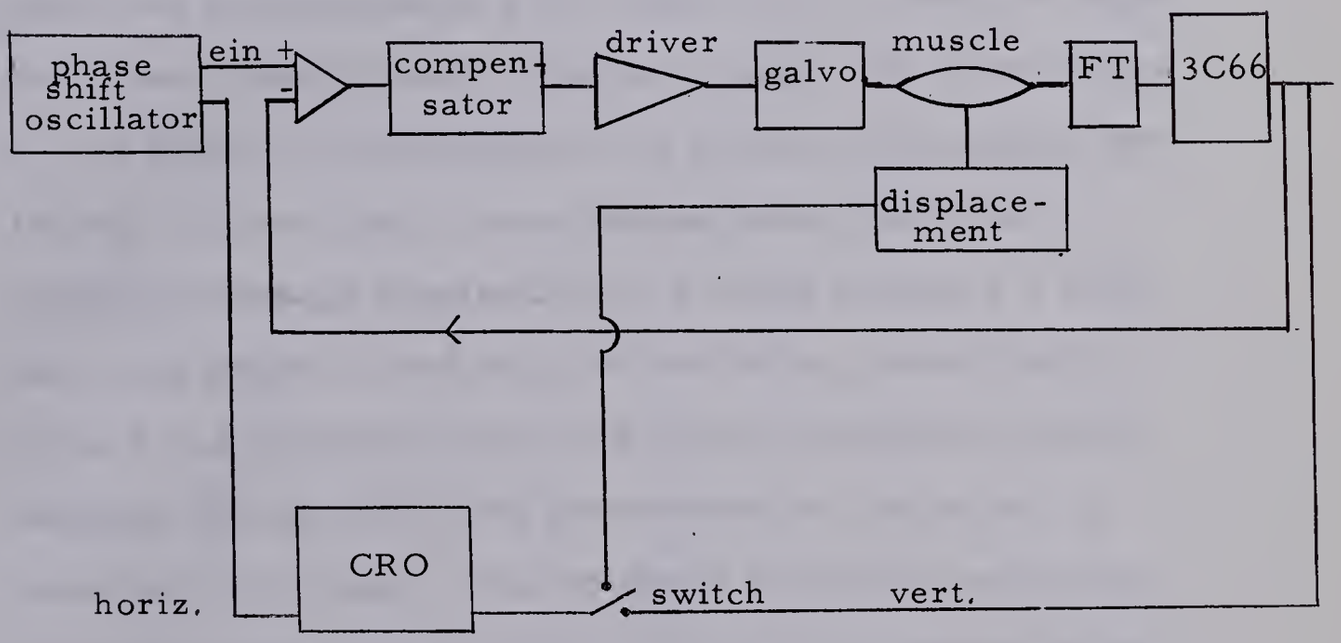

Figure 17. Block Diagram of Experimental Arrangement Used to Measure the Mechanical Characteristics of Muscle

Using the arrangement shown in Figure 17, frequency response curves were obtained for several muscles. Some initial tension was applied to the muscle and the magnitude of the force variation was kept small so that the nonlinear effects of muscle compliance would have little effect on the variation (i.e., the compliance would have essentially a constant value over

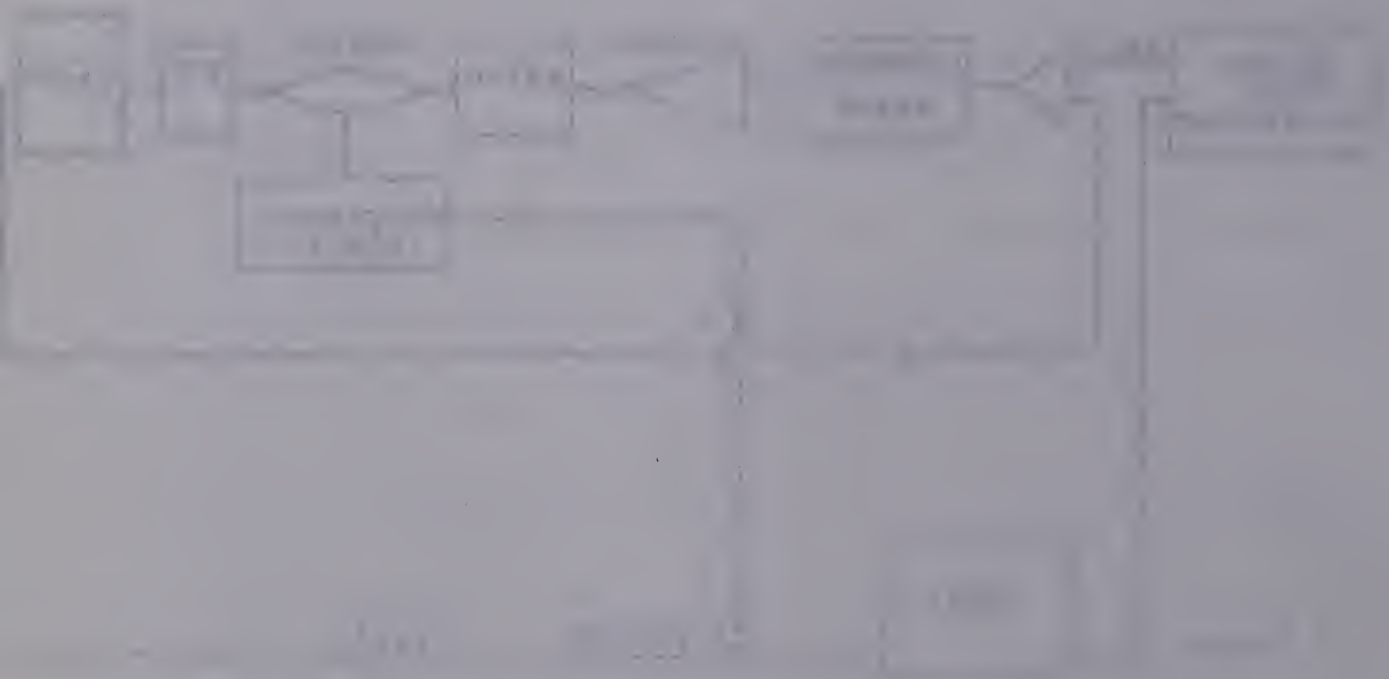

the complete variation). The nonlinear characteristic of muscle compliance is discribed by Buchthal (2) and Wilkie (12).

4.8 RESULTS

The measurements on muscle yielded the magnitude and phase shift of the applied force and the resulting displacement with respect to the reference voltage (input).

Normalized curves of $\frac{X(j\omega)}{F(j\omega)}$ are plotted in Figures 18 and 19. Curve 1 was obtained using frog's sartorius muscle which was prestretched to a test length of 1.13 times the length in the body; while in curve 2 the same muscle was prestretched to 1.35 times the initial length. The weight of this sample was 150 mg. Curves 3 and 4 were obtained using frog's semi-tendinosus muscles prestretched to a length of about 1.1 times the initial length and weighing 100 and 94 mg. respectively. Curve 5 was obtained using a toad's semi-tendinosus muscle weighing 250 mg. which was prestretched to a length of 1.1 times the initial length. The estimated resonant frequency of this sample was about 200 hertz. Curve 6 was obtained using frog's semi-tendinosus muscle weighing 110 mg. and prestretched to a length of 1.15 times its initial length. The above results were obtained using a sinusoidal force less than 9.8×10^{-3} newtons peak to peak.

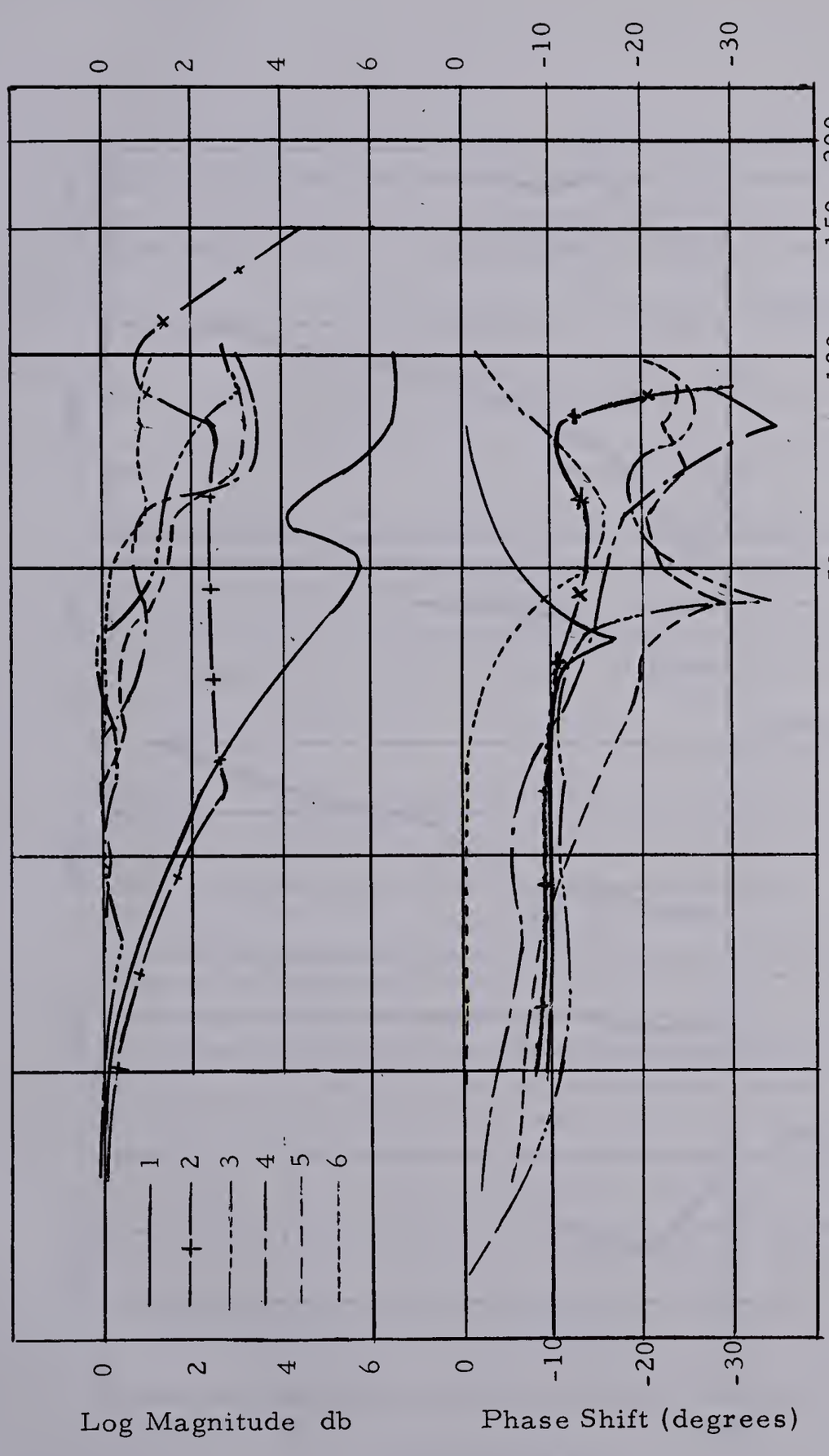

Figure 18. Frequency Response Curves Showing Results Obtained From the Measurement of the Muscle Transfer Function

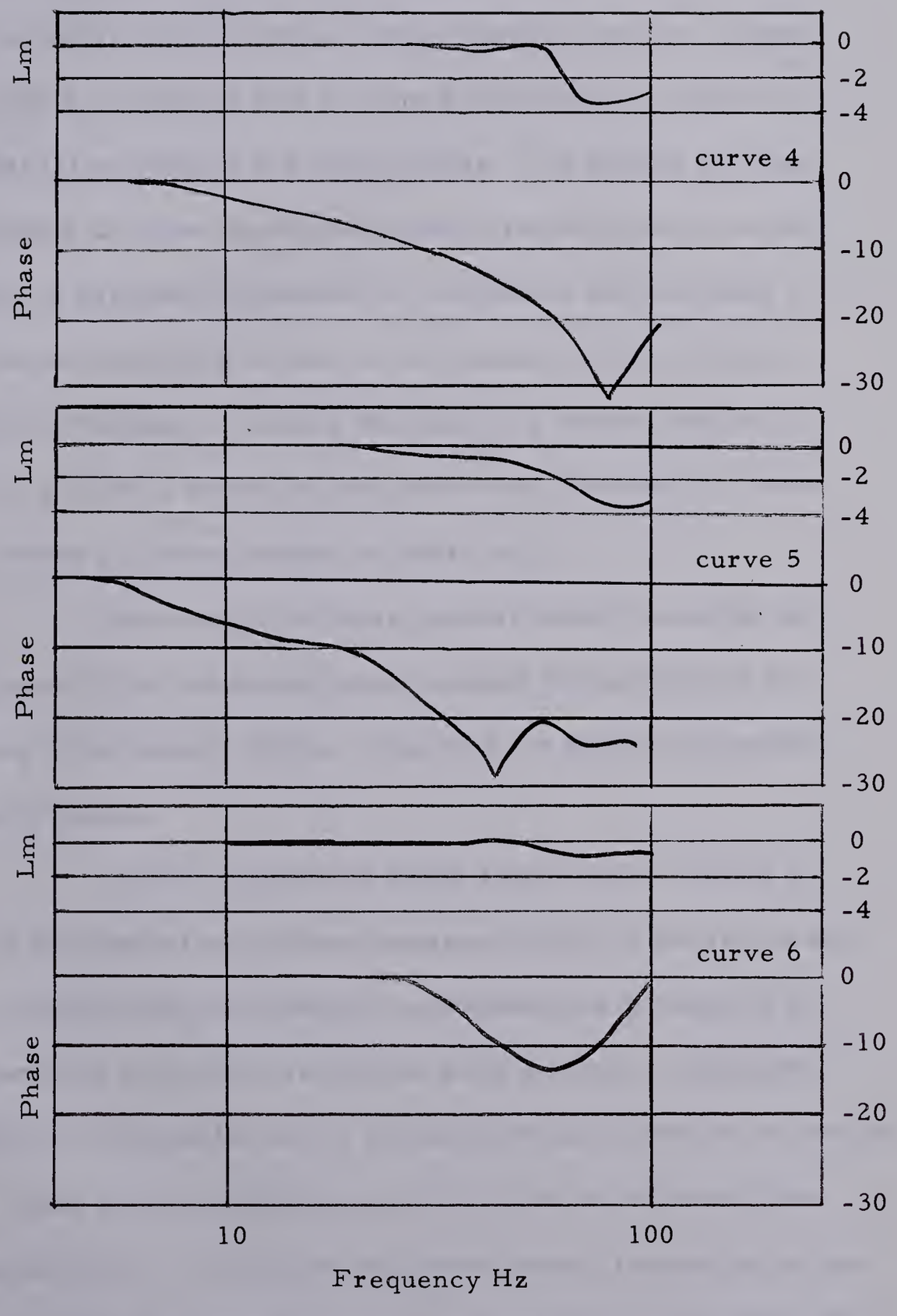

Figure 19. Frequency Response Curves of Typical Muscle Transfer Function Measurement Results

4.9 DISCUSSION

The results obtained from the measurement of the mechanical transfer function of muscle shown in Figures 18 and 19 do not represent any simple linear transfer function. These results do not compare with the linear relationships obtained by Buchthal (2) on bundles and single fibres. The results obtained by Buchthal (2) show clearly one corner frequency which would be due to a parallel combination of compliance and damping. No such distinct corner is evident in the results shown in Figures 18 and 19. However at certain frequencies a sudden change in phase is evident in nearly all the tests done. Buchthal (2) however, shows no measurements of phase shift.

One reason for these unusual results could be that compliance of the connective tissue masked the compliance and damping of the muscle fibres. This does not explain the sudden change in phase.

Another possibility which seems quite unlikely is that the mechanical oscillation causes excitation of the fibres and hence, contraction. An attempt to eliminate this possibility by prestretching the muscle so that the actin and myosin filaments no longer overlap failed due to the large forces needed to accomplish this. Under these prestretched conditions the muscle would no longer contract. If excitation did indeed exist, tetanus might explain the change in phase; however, the results do not confirm this.

CHAPTER V

EVALUATION OF SYSTEM

5.1 DIRECT COUPLED CASE

A. Transient Response

A 5 hertz square wave was applied to the compensated system with the open loop gain set at 10. The system was direct coupled and compensated as shown in the frequency response curves in Figure 11. The square wave response is shown in Figure 20. The damping ratio for this gain is calculated to be about .45.

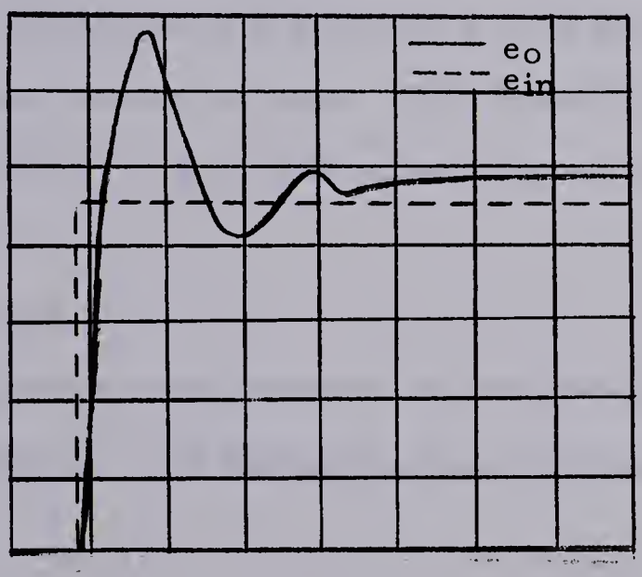

Figure 20. Transient Response of Direct Coupled System

B. Steady State Error

With the system gain equal to 10 the static error coefficient of the type zero system K_o is defined as:

$$K_o = \lim_{s \to 0} K\ G(s)\ \ G_{c1}(s)\ G_{c2}(s)\ G_{c3}\ (s).$$

For the system in question, $K_o = 10$ since $K = 10$.

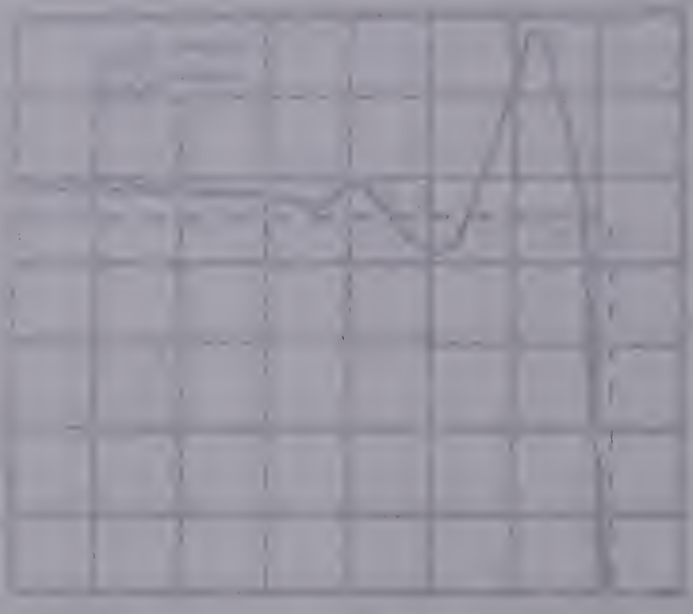

The steady state error is given as follows:

$$e_{ss} = \frac{R}{1 + \underset{s \to 0}{\text{Limit}} \; G(s) \quad G_c(s)}$$, where $e_{ss} = \frac{100\%}{1 + K_o}$

$= 9\%$.

The steady state error measured from the square wave input was also about 9 percent. The gain was increased to 15 and the steady state error, both measured and calculated, was about 6 percent. This mode of operation was poor for frequencies over 30 hertz since the damping ratio was very low resulting in a large resonant peak.

C. Bandwidth

The bandwidth of the system with a gain of 10 is 70 hertz. A resonant peak is evident. The bandwidth may be increased by an increase in gain with an associated increase in the resonant peak.

D. Distortion

Distortion measurements on the system were made at 20 hertz and 50 hertz. The distortion measurements are given below in Table I.

Frequency	Open Loop Distortion %	Closed Loop Distortion %
20 hertz	3.5	.7
50 hertz	4.5	1.8

Table I. Comparison of Closed and Open Loop Distortion.

E. Drift

In the design of the circuit, silicon transistors were used and the stages were alternate pnp and npn to minimize

temperature drift. The force transducer was used in the four arm bridge configuration in order to minimize temperature effects. No measurements of temperature sensitivity were made because the final system was to operate closed loop, and the carrier amplifier and transducer, which contribute to the overall drift, were purchased items.

5.2 MUSCLE COUPLED CASE

A. Transient Response

The effect of a 5 hertz square wave on the system with a gain of 10 is shown in Figure 21.

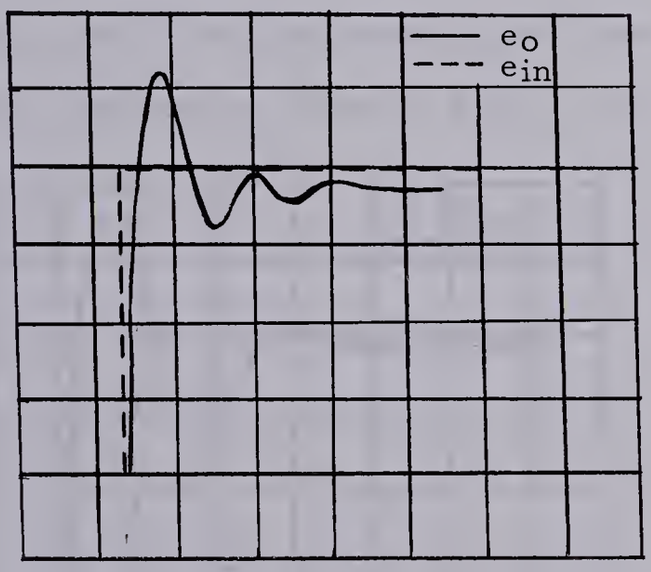

Figure 21. Transient Response of Muscle Coupled Cases

The damping ratio was calculated to be .34.

B. Steady State Error

The steady state error to a step is the same as in the direct coupled case which is 9 percent.

C. Bandwidth

The -3 db point with a gain of 10 was 65 hertz and the resonant peak was measured to be 5 db at 50 hertz. The results of these measurements are given in Table II.

D. Distortion

Distortion measurements were again made on the system at 20 hertz and 50 hertz.

Frequency	Open Loop Distortion %	Closed Loop Distortion %
20 hertz	6.5	1
50 hertz	7	4.7

Table II. Comparison of Closed and Open Loop Distortion.

5.3 LAG NETWORK AT LOWER FREQUENCY

A. Transient Response

For a gain of 14, the damping ratio was calculated to be .50. The step response is shown in Figure 22.

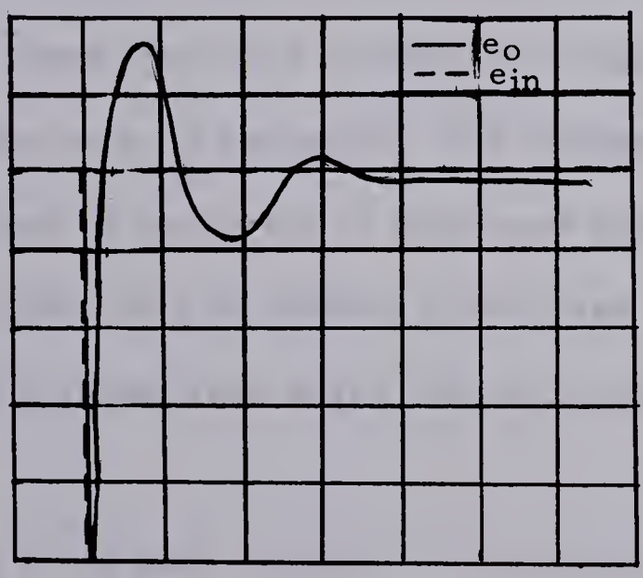

Figure 22. Transient Response with Lag Network at Lower Frequency

B. Steady State Error

The steady state error for this system was measured to be about 6 percent.

C. Bandwidth

The bandwidth for this case was about 70 hertz. The resonant peak was about 4 db.

D. Distortion

The open loop distortion is 5 percent as compared to .9 percent closed loop at 20 hertz.

5.4 CONCLUSION

The original system which was very unstable was compensated using two bridged-T networks and one lag network. The effect of this compensation resulted in the steady state error of 6 to 7 percent. This did not meet the original specification of 2 percent. If a low steady state error is required, the lag network could be set to a lower frequency resulting in a higher gain but with a resulting decrease in bandwidth. The damping ratio likewise depends on gain and, if the system is to be used with a step function as the input, the gain could be lowered to decrease the bandwidth and to increase the steady state error with an improvement in the damping ratio.

One of the main reasons for the design of this system was to decrease the distortion of the applied force due to muscle nonlinearity. The amount of improvement is dependent on the gain and, from the results of measured distortion, a definite improvement is seen.

For use, at up to 30 or 40 hertz, with a sinusoidal input the system may be operated at higher gains. (A sinusoidal input may be used in the study of mechanoreceptors.)

5.5 RECOMMENDATIONS

As suggested in Chapter I, it was found that the equipment limited the achievement of the desired specifications. Since the system does not quite meet all specifications outlined in Chapter I, some suggested improvements could be the use of a faster galvanometer and as the force transducer, the use of a unit with a much higher resonant frequency and a better damping ratio.

BIBLIOGRAPHY

1. Brown, R.G. & Nilsson, J.W. Introduction to Linear Systems Analysis. New York: John Wiley & Sons, 1962.

2. Buchthal, F. Det KGL Danske Videnskabernes Selskab. Volume 17, 1942-1943.

3. Chapman, K.M. Campaniform Sensilla on the Tactile Spines of the Legs of the Cockroach; Journal of Experimental Biology. Volume 42 # 2, April 1965.

4. Chapman, K.M. & Smith, R. A Linear Transfer Function Underlying Impulse Frequency Modulation in a Cockroach Mechanoreceptor; Nature. Volume 197, 1963.

5. Chandaket, P. & Rosenstein, A.B. Notes on Bridged-T Complex Conjugate Compensation and Four-Terminal Network Loading; AIEE Transaction, Applications and Industry. July, 1959.

6. D'Azzo, J.J. & Houpis, C.H. Feedback Control System Analysis and Synthesis. New York: M^{c}Graw-Hill & Company, 1960.

7. Huxley, H.E. Electron Microscope Studies on the Structure of Natural and Synthetic Protein Filaments from Striated Muscle; Journal of Molecular Biology. Volume 7, Sept. 1963.

8. Huxley, H.E. Structural Arrangement and the Contraction Mechanism in Striated Muscle; Proceedings of the Royal Society. Series B, Volume 160, Oct. 1964.

9. Huxley, A.F. The Links Between Excitation and Contraction; Proceedings of the Royal Society. Series B, Volume 160, Oct. 1964.

10. Jewell, B.R. & Wilkie, D.R. An Analysis of the Mechanical Components in Frog's Striated Muscle; Journal of Physiology. Volume 143, 1958.

11. Kuo, B.C. Automatic Control Systems. New Jersey: Prentice-Hall Inc., 1962.

12. Wilkie, D.R. The Mechanical Properties of Muscle; British Medical Bulletin. Volume 12, 1956.

APPENDIX I

In order to obtain the frequency response curves of the system, an amplifier was built to drive the galvanometer. The output stage consisted of a Darlington arrangement used as an emitter follower. The input stage was a differential amplifier. A circuit diagram is shown in Figure A-1.

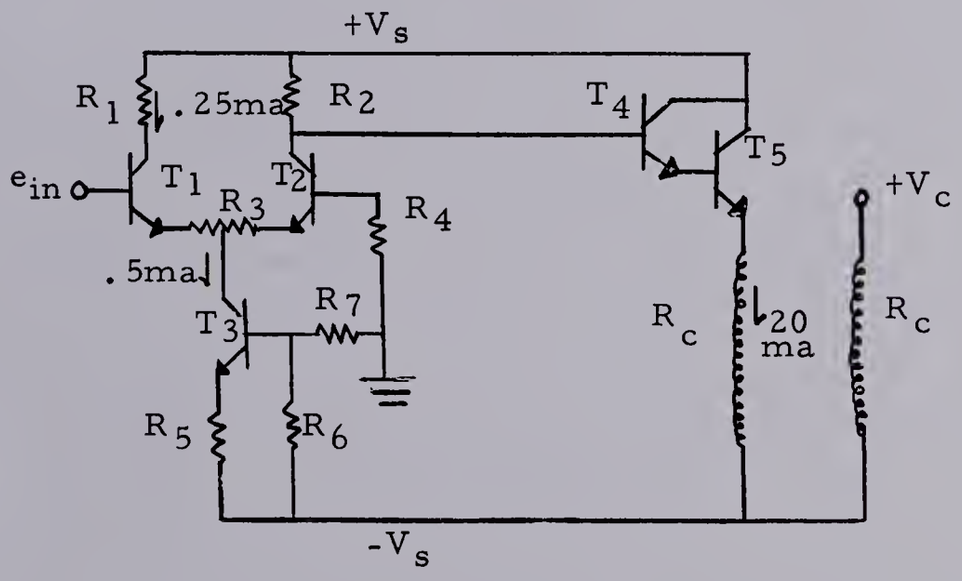

T_1, T_2, T_3, T_4 = TI 495

T_5 = TI 487

$R_1 = R_2 = 33K$ $\qquad$ $R_7 = 5.6K$

$R_3 = 2K$ $\qquad$ $R_6 = 12K$

$R_c = 1.5K$ $\qquad$ $R_5 = 12K$

Figure A-1. Driver Circuit Used to Obtain the Frequency Response Curves of the System

The output impedance of the configuration is given by the expression $Z_{out} \approx h_{ib_5} + \frac{R_L}{h_{fe_4} h_{fe_5}}$ where $h_{ib_5} = \frac{26mv}{I_{E5}} + 1.5 \approx 2.8$ ohms.

Therefore $Z_{out} \approx 10$ ohms.

The single ended gain of the circuit is given by the following expression:

$$A_v = \frac{R_L}{h_{ib_1} + h_{ib_2} + R_E} \approx 15.$$

APPENDIX II

The compensators as designed in Chapter 3, and the driver amplifier shown in Appendix I, were incorporated into a single amplifier. Also included in the circuit was a differential amplifier needed to provide the error signal.

INPUT STAGE

To provide an error signal to drive the galvanometer a differential amplifier was used. It was designed with a temperature compensated current source and emitter resistors to aid in the D.C. balance of the system. The input stage is shown in Figure A-2.

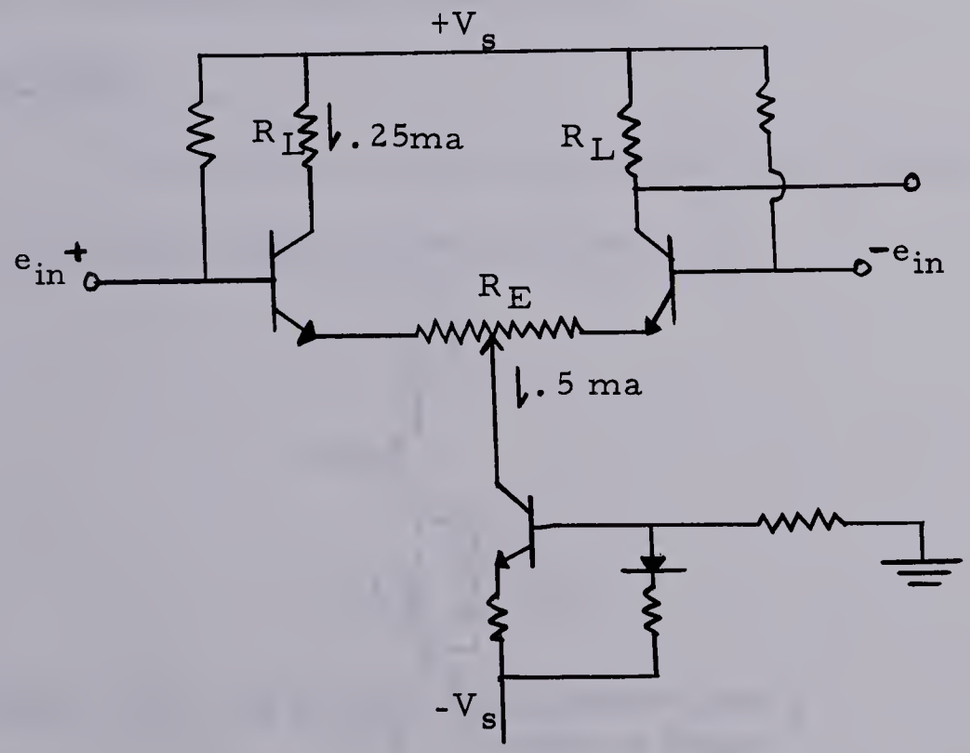

Figure A-2. Circuit Diagram of Input Stage

The voltage gain for a single ended output is given by:

$$A_v \approx \frac{R_L}{2h_{ib} + R_E}.$$

In the actual circuit the voltage gain is approximately 1.2 for an operating current of .5 ma.

The single ended input impedance is given by:

$$Z_{in} = h_{fe} \ (2h_{ib} + R_E) \ // \ R_B$$

$$\approx 8.4 \text{ megohms.}$$

IMPEDANCE MATCHING OF COMPENSATION

In order not to affect the transfer function of the bridged-T compensators the input and output impedances were matched using emitter followers. Alternate pnp and npn stages were used to minimize temperature effects.

LAG NETWORK

The lag network was incorporated into a common emitter transistor stage as shown in Figure A-3.

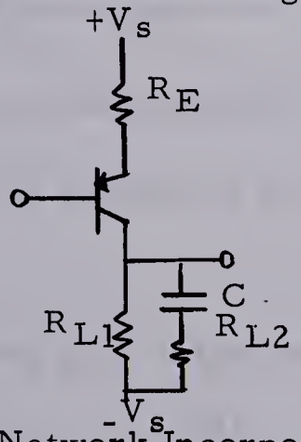

Figure A-3. Lag Network Incorporated Into a C.E. Transistor Stage

The transfer function for this circuit is given by the expression for voltage gain as $A_v \approx \frac{R_L}{R_E + h_{ib}}$, but $R_L = R_{L1} // R_{L2} + \frac{1}{sC}$ so that $A_v \approx \frac{1}{R_E + h_{ib}} \left(\frac{s + \frac{1}{R_{L2}C}}{s + \frac{1}{R_{L1} + R_{L2}C}} \right)$.

Gain of the stage is 2.2 at D.C.

OPERATIONAL AMPLIFIER STAGE

In order to provide additional gain to the system which could be adjusted without shifting the D.C. level a simple operational amplifier was used. A circuit diagram is shown in Figure A-4.

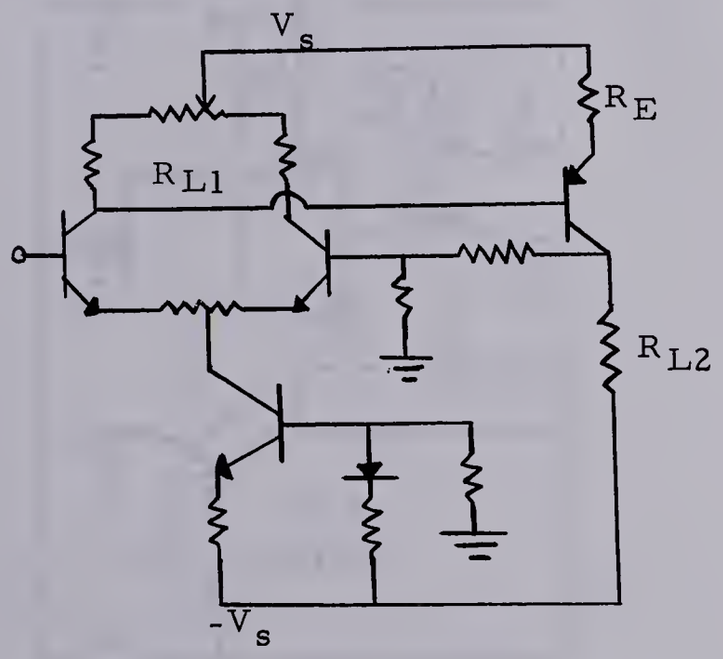

Figure A-4. Operational Amplifier

The operating current of the differential stage was set at .5 ma.

The open loop gain of this amplifier is given as follows: $A_v = \frac{R_{L1}}{2h_{ib} + R_E} \times \frac{R_{L2}}{R_E} \approx 450.$

The diode was again used to temperature compensate the current source.

This amplifier was then followed by the driver stage which is discussed in Appendix I. A complete circuit diagram is given in Figure A-5.

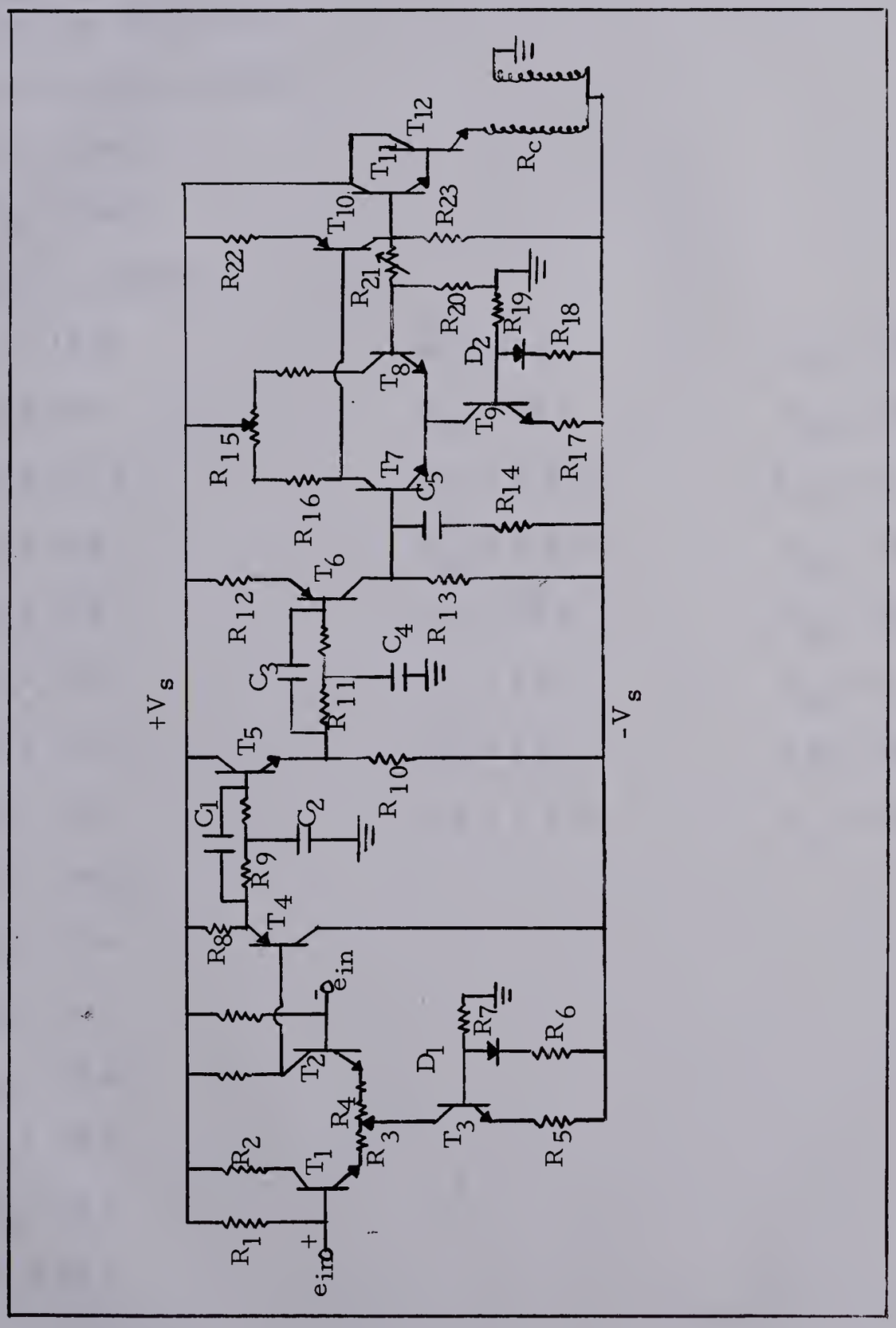

Figure A-5. Circuit Diagram of Complete Circuit

LIST OF COMPONENTS

T_1, T_2, T_7, T_8 = 2N3707

T_3, T_5, T_9 = 2N3705

T_4, T_6, T_{10} = 2N3703

T_{11} = TI415

T_{12} = TI487

D_1, D_2 = 1N1020

R_1 = 15 M

R_2 = 27 K

R_3 = 2.7 K

R_4 = 20 K

R_5 = 12 K

R_6 = 12 K

R_7 = 5.6 K

R_8 = 15 K

R_9 = 15 K

R_{10} = 39 K

R_{11} = 5.6 K

R_{12} = 6.8 K

R_{13} = 15 K

R_{14} = 1 K

R_{15} = 2 K

R_{16} = 4.7 K

R_{17} = 12 K

R_{18} = 12 K

R_{19} = 5.6 K

R_{20} = 10 K

R_{21} = 1 M

R_{22} = 2.2 K

R_{23} = 33 K

R_c = 1.5 K

C_1 = .001 uf

C_2 = .5 uf

C_3 = .1 uf

C_4 = .33 uf

C_5 = .68 uf

$+V_s$ = 20 v

$-V_s$ = 20 v